UNDERSTANDING GRANULATION OF CERAMIC POWDERS: CASE STUDY (Al_2O_3)

by

Mohamed Ahmed Abdellah Omar

Submitted to the Graduate School of Materials Science and Nanoengineering

in partial fulfillment of the requirements for the degree of Master of Science

Sabanci University

February 2023

Mohamed Ahmed Abdellah Omar 2023 ©

All Rights Reserved

ABSTRACT

UNDERSTANDING GRANULATION OF CERAMIC POWDERS: CASE STUDY (AL_2O_3)

Mohamed Ahmed Abdellah OMAR

Materials Sciences and Nano Engineering, Master Thesis, February 2023

Supervisor: Prof. Dr. Mehmet Ali GULGUN

Keywords: Granulation, Spray dryer, Atomizing, Flowability, Crushability.

Aluminum oxide, also known as alumina, is a ceramic material with a wide range of commercial applications, including the production of bulletproof shields. To improve the properties of alumina, such as toughness, hardness, and density, researchers have focused on improving the processing of the material.

This study investigates the granulation process and properties of aluminum oxide (alumina) granules, with a focus on improving flowability, particle size, and crushability. The spray drying technique is explored as a means of controlling the properties of the granules through various parameters. The characteristics of the granules produced under

controlled processing conditions were studied using a scanning electron microscope, particle size analysis device, flowability repose angle test, and uniaxial pressing tests. The results showed an increase in granule size from 17.7 μm to 29.9 μm when collected from different positions in the drying chambers. The study presents the influence of various experimental parameters on the outcome of the spray drying of nanometric alumina powders. Slurry as well as spray drying condition parameters influenced the granule size and granules flow properties. Certain parameters emphasized in the literature were observed to have minimal influence on properties in contrast to literature reports.

ÖZETİ

SERAMIK TOZLARIN GRANÜLASYONUNUN ANLAŞILMASI: (AL_2O_3) ÖZELINDE ÇALIŞMALAR

Mohamed Ahmed Abdellah OMAR

Malzeme Bilimi ve Nano-mühendislik, Yüksek Lisans Tezi, Şubat 2023

Danışman: Prof. Dr. Mehmet Ali GÜLGÜN

Anahtar kelimeler: Granülasyon, Sprey kurutma, Atomizasyon, Akışkanlık, Kırılabilirlik.

Alümina olarak da bilinen Alüminyum Oksit, kurşun geçirmez kalkanların üretimi de dahil olmak üzere geniş bir ticari uygulama yelpazesine sahip seramik malzemedir. Aluminanın sertlik, dayanıklılık ve yoğunluk gibi özelliklerini geliştirmek için araştırmacılar malzemenin işlenmesini iyileştirmeye odaklanmışlardır.

Bu çalışma, alüminanın akışkanlığını, parçacık boyutunu ve granüllerin kırılabilirliğinin geliştirilmesine odaklanarak, alüminyum oksitin (alumina) granülasyon sürecini ve özelliklerini araştırmaktadır. Sprey kurutma tekniği, granüllerin çeşitli

parametreler aracılığıyla özelliklerinin kontrol edilmesi için incelenmiştir. Kontrollü işleme koşullarında üretilen granüllerin özellikleri, Taramalı elektron mikroskobu SEM, parçacık boyutu analiz cihazı, akışkanlık repoz açısı testi ve uniaxial pres testleri kullanılarak incelenmiştir. Sonuçlar, kurutma odalarındaki farklı konumlardan toplandığında granül boyutunda 17,7 μm'den 29,9 μm'ye kadar bir artış olduğunu göstermiştir. Çalışma, nanometrik alumina tozlarının sprey kurutma üzerindeki çeşitli deneysel parametrelerin sonuclar üzerindeki etkisini sunmaktadır. Çamur Özellikleri ve sprey kurutma prosesinin parametreleri granül boyutunu ve granüllerin akış özelliklerini etkilemiştir. Literatürde vurgulanan belirli parametrelerin, özellikler üzerinde minimum etkiye sahip olduğu görülmüştür.

ACKNOWLEDGMENT

To my GOD and that drawn FATE for me…

To my beloved FAMILY and my WIFE….

My FRIENDS…

To my TEACHER and COLLEAGUES…

TABLE OF CONTENTS

List of tables

List of figures

1. Introduction

1.1. Ceramic processing

The preparation of ceramics involves several stages in order to achieve the desired electrical, mechanical, chemical, and physical properties. These stages are guided by principles of thermodynamics, quantum mechanics, and mechanics. The diagram below (figure 1) provides a brief overview of the ceramic processing stages. Our focus in this study was on the mixing and forming process.

Figure 1. Ceramic processing diagram

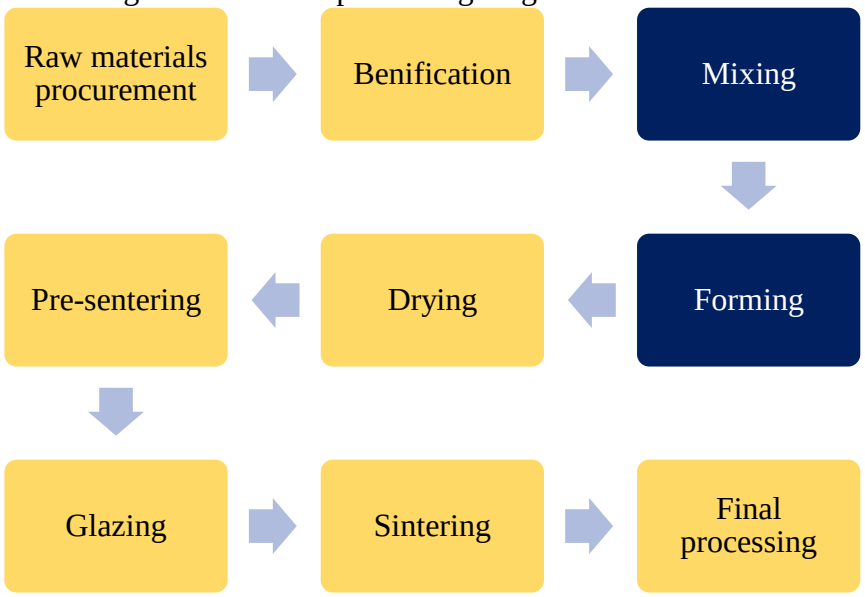

The process of transitioning ceramics from natural materials to practical applications involves the following steps:

I. **The raw materials procurement process** involves applying chemical synthesis to mined natural resources. A ceramic raw materials manufacturer typically works with feldspar, silica, sand, flint, silicates, quartz, and aluminosilicates.

II. **Beneficiation** is a process that takes place at the mining site or at a processing facility before the raw materials are transported to a ceramic manufacturing company. This stage involves using various techniques to reduce the materials to small particles, such as milling, crushing, and grinding. The materials are then purified by washing with water and filtering to remove impurities. Other methods, such as acid leaching and extracting magnetic impurities, may also be used to purify the materials. The final steps in the beneficiation process are classification and packing.

III. **The process of mixing** involves preparing a powder that is stable both chemically and physically for the forming process. During mixing, various additives such as binders, plasticizers, lubricants, surfactants, antifoaming agents, and deflocculants are carefully added in specific amounts and types. The selection of these components, even if some are absent, is an area of research for each material.

Between the previous and following stages of the ceramic production process, we focused on spray drying alumina powder and preparing granules in order to address any issues with the product from the previous process and to facilitate the following stages. Our main concerns were adjusting the spray drying process and determining the relationship between different parameters. The goal was to produce a final granule with the desired properties, which were tested through measures of flowability, crushability, and particle size analysis. Ultimately, we aimed to understand the effect of individual parameter values on key properties.

IV. **Forming:** This stage produces the green body, which can be made using traditional or non-traditional processes. Traditional forming examples include dry pressing uniaxially, wet/dry isostatically pressing, slip casting, and plastic forming, while non-traditional processes include hot pressing, vapor deposition, injection molding, sol-gel processing, and gel

casting. Afterward, green machining is performed to smooth out rough surfaces and shape the final product according to specifications.

V. **Drying:** This stage takes place in a tunnel kiln using a convection air drying mechanism. The drying process is controlled to be quick and ensure that there is no differential shrinkage of the body.

VI. **Pre-sintering:** In this stage, the body is further dried by heating it below the sintering temperature. This process decomposes and evaporates binders and additives.

VII. **Glazing:** In this stage, a coating of raw materials with low melting temperatures is applied to the body. These materials serve as a decorative layer after sintering, providing color and a waterproof surface. This step is not required for all applications.

VIII. **Sintering:** This process involves densifying the bulk through the application of pressure and heat, reaching almost two thirds of the material's melting temperature. There are several factors to consider in the sintering process, such as the particle size of the material, the density of the green body, and the shape of the product. Key parameters that affect the sintering process include temperature, time, pressure, and atmosphere, and their values vary depending on the material and required application.

During sintering, the product goes through several stages: the initial stage forms a low-density, porous product; the second intermediate stage produces a high-strength product with fine grains; and the third stage produces a product with increased resistance to creep, made up of coarse grains.

IX. **Final Processing:** This stage involves various processes to finish the product, including coating, machining, annealing, polishing, and chemical grinding, to meet dimensional tolerances.

The final product of ceramics production is a brittle, dense, sintered body, but achieving this requires careful modification of each process and its parameters within the

applicable range. Researchers have studied the various parameters involved in these processes and their effects on the properties of the final product.

This study specifically focuses on the preparation of granules through spray-drying of alumina powders, which is a part of the powder preparation and mixing stage preceding the forming process. The following sections will first define powders and granules, then provide a detailed explanation of the spray drying mechanism.

1.2. Powder

The powder is defined as a collection of small, solid particles with a size range of nanometers or microns[1]. The physical properties of the powder are determined by the nanostructure of each particle and its chemical composition. Ceramic powders, in particular, are known for having similar physical properties to the final ceramic product[2].

When selecting a raw material for a ceramic application, it is important to carefully consider the properties of the powder. Ceramics have high melting temperatures that can be difficult to reach and handle. One important property to consider is flowability, as the powder must be able to flow like a liquid in order to fill the mold evenly and not have an irregular solid morphology that does not fit well in molds[2]. Powders are characterized according to table 1 [3].

Table 1. powder characteristics[3]

Particle and Powder Characteristics	
Characteristics of a Single Particle	Powder Characteristics
Size	Particle size distribution, an average of particle size, Standard deviation in particle size.
Density	Average particle density, bulk density, tap density.
Shape	Characteristic particle shape
Composition	average composition.
Surface area (geometric)	Specific surface area.
Phases and crystallinity	Average crystallinity and phase content.
Yield strength	Compressibility or compaction behavior.
-	The flow rate or repose angle of flowability.
Surface energy	-

Ceramics are known for their brittleness, which can significantly impact the properties of the final product. For example, using a powder with a broad range of particle sizes may result in a dense green body, while using a powder with smaller particle size distribution may have negative consequences. This underscores the importance of carefully selecting the powder before sintering[3].

To achieve high strength and brittleness in ceramics, it is important to use powders with fine grains and a dense microstructure that is free of impurities. Incomplete densification can be a major issue, so it is necessary to carefully control the density of the green or sintered bodies. To do this, it is essential to consider the sintering process when selecting the starting powders[2]. Simply using powders with small average particle sizes

is not enough, as these particles may have irregular shapes and rough surfaces that hinder flowability. In these cases, it may be necessary to use granules instead[1, 2].

1.3. Granules

Granules are small, controlled agglomerates that can range in size from microns to sub-microns. One of the benefits of using granules is that they allow for the addition of binders, plasticizers, and lubricants to alter the properties of the powder. This can help to control the green strength of the material. Granules come in a variety of morphologies, such as sphere or donut-like shapes, and may contain pores, water, binders, and lubricants.

Granules compared to powders are preferred for many reasons[1].

- Preventing weight density segregation while pressing the bulk material.
- Avoiding segregation of one component in composite ceramics figure 2.

Figure 2. Segregated powder. And granules/powder differences[1].

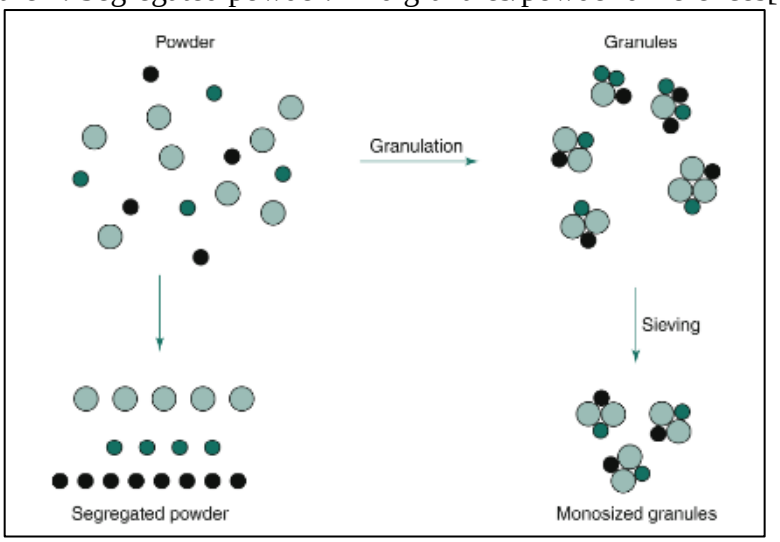

- Powders are irregular rough surfaces of solid particles. Thus, cohesive property results in between particles decreasing the flowability.

- Granules are relatively larger and smoother in surfaces. Which in its turn increases the flowability.
- Improvement of compaction is another advantage of having granules. The structure of the granules is the reason for that property. During granulation and specifically in the drying stage, solute migrates with the binder to the outer shell. Then granules with binder-rich outer layers are the result.

  A binder-binder bond between granules enhances the consolidation of weak bonding materials.
- Granules have less dust which reduces the hazards that result from handling.
- On a large scale, granules are packed relatively in less volume per unit weight compared to powders.

Granules and powders in the micron or nanometer range serve as a link between bulk materials and atomic or molecular structure. The chemical, mechanical, and physical properties of these particles are determined by their surface area. For example, the flowability and compaction of granules and agglomerated powders during the filling of a die for dry pressing can have significant effects on the properties of the green body[4].

The properties of the sintered body are also influenced by granules and powders. Therefore, it is important to consider how granules are made and which materials are used in their preparation. These issues will be addressed in the following pages.

1.4. Spray drying

Spray drying is a technique for preparing ceramic powders that involves the formation of spherical granules through the agglomeration of small particles[5]. This method has gained popularity in the pharmacy and ceramics sectors, and it works by applying instant, sudden heat to a droplet to remove moisture and produce a final granule [6-9].

The spray drying process involves precise control of the working environment, including factors such as outlet temperature, inlet temperature, pressure, fan speed, and feeding rate. It also requires careful preparation and mixing of the slurry, as well as the selection of appropriate solvents and solutes. The final step of spray drying involves collecting the powders according to the design of the machine.

In addition to the biomedical and food industries, ceramics have also benefited from the theoretical and practical advantages of spray drying. For example, high compaction and good mechanical properties of green body and sintered density have been achieved, thanks to the high flowability of granules produced using a spray dryer. This technique allows for the precise control of binder levels in the slurry, both chemically and through the use of physical electrostatic deflocculation. As a result, ceramics processing offers a range of parameters that can be adjusted for each material.

The morphology of granules has been the subject of much investigation, with researchers examining the effects of initial solid content on granule shape [8, 10-12].

However, these studies have primarily focused on the qualitative and quantitative selection of binders and dispersion agents or the dispersion state without deflocculant[5]. These ingredients will be discussed in wider detail later in this study.

The use of a spray dryer leads to the production of granules with high flowability, resulting in improved green density. It is also known that geometrically rounded or donut-shaped powders have a high flowability property, which can lead to improved homogeneity in powder distribution, easier pressing and extrusion, and more precise final dimensions in simple or complex products.

While spray drying is a promising technique for ceramics processing, there are still many unknown correlations that require further investigation in order to optimize granule production. One obstacle is the effect of Van der Waals forces, which can reduce flowability for powders with large particle sizes. In addition, the particle size distribution of the powder can influence the grain growth stage during sintering.

The glass transition of polymers included in the granulation slurry can also affect the range of machine parameters that can be used. This means that adjusting the chemicals and their concentrations in the solution is another important consideration. This study aims to understand how to control granule size and what factors influence it, as well as to examine the effects of these factors on the sintered product.

The mechanism used in a spray dryer depends on the surface area of the ejected solution as droplets, which are then dried considering factors such as surface tension, viscosity, and density. Choosing the appropriate chemical ingredients is an important part of preparing feed solutions, as it can directly affect the characteristics of the resulting material. Atomization then occurs, resulting in the formation of dried particles. These dried particles are collected in the collection bottle[13]. The working principle of spray dryer

- Atomizing slurry.
- Drying droplets.
- Collecting granules.

Figure 3. Spray dryer components[14]

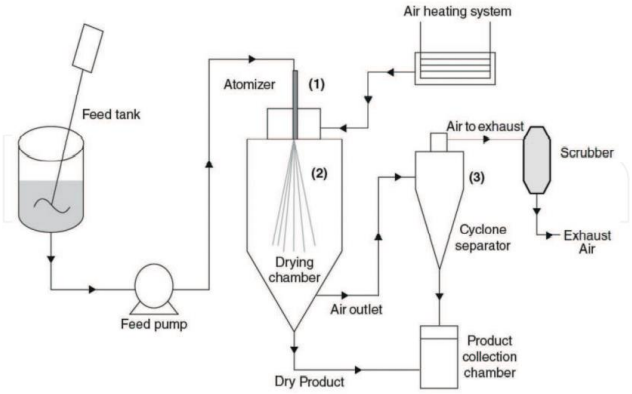

1.4.1. Atomizing

Atomization, which involves the efficient transfer of mass and heat, is achieved through the breaking up of droplets of the initial feed solution. This can be done using the designed nozzle of a spray dryer, which facilitates the instantaneous evaporation of the droplets. The nozzle is a critical component that determines the final characteristics of the granules rheology, as it influences the drying of the droplets[13].

Historical investigations into the solution feeding rate, droplet size distribution, and shape have resulted in mathematical equations that can be used to understand and optimize atomization conditions, considering the inherent errors and defects of the process. These equations consider the evaporation environment and the design of the nozzle, which can vary for different research and industrial purposes.

Joseph Plateau was the first to observe and characterize the instability of a liquid jet as it falls vertically under the force of gravity. He found that the surface area of the liquid increases as it reaches a critical length, at which point it no longer maintains its cylindrical shape and instead breaks up into droplets. This process of liquid instability is illustrated in figure 4.

Figure 4. Droplet formation[6]

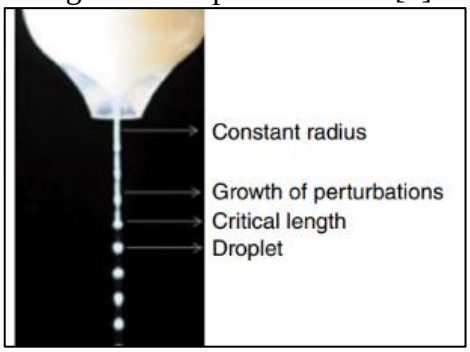

Lord Rayleigh is known for his “Liquid jet theory”, which builds on the work of Joseph Plateau and examines the break-up of non-viscous liquids in a horizontal flow state. He developed a mathematical function to understand this process of a laminar jet, finding that the optimum oscillation wavelength is 4.51d, where d is the initial jet diameter. The length of the cylinder before mismatch was = 4.51d which was broken into

a separated droplet with an equal spherical volume, which can be proportional to the jet's initial diameter according to equations 1, 2. A visualized schematic shows more details in figure 5.

$$4.51d \times \left(\frac{\pi}{4}\right) d^2 = \left(\frac{\pi}{6}\right) D^3 \quad (1)$$

Hence,

$$D = 1.89d \quad (2)$$

Figure 5. Horizontally droplet formation[14]

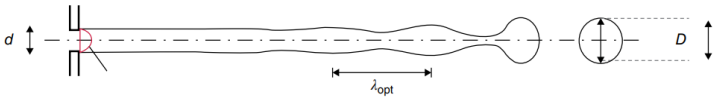

Back to the history of spray dryers, lots of studies paid attention to the relation between the nozzle diameter, droplet type, size, and volume. That is why investigations of the droplet behavior must be also introduced by the physical properties of the feeding solution of the specimen. therefore, considering surface tension and inertial forces by Rayleigh was not enough to explain the effect of the feeding solution's viscosity and atomization gas.

Weber had a further investigation into that and he showed:

- At zero relative velocity between the liquid jet and the surrounding air he obtained λopt = 4.44d
- A shortening of the optimum wavelength occurs because of the air friction.
- With relative velocity = 15 m/s, the optimum wavelength λopt reached 2.8d and resulted in a droplet of 1.6d diameter.

To sum up, increasing the relative velocity resulted in a smaller wavelength of the broken jet, and vice versa.

Finally, Ohnesorge proposed a function that includes all the related critical parameters for atomization in terms of viscosity, density, surface tension, and jet size. A relation between Reynolds and Weber observations is calculated to get a dimensionless Ohnesorge number (Oh) at equation 3.

$$Oh = \frac{\sqrt{We}}{Re} = \frac{\mu}{\sqrt{\rho\sigma L}} = \frac{Visxous\ forces}{\sqrt{(ineria \times surface\ tension)}} \quad (3)$$

where:

(We) is the Weber number; (Re) is the Reynolds number; (μ, ρ, and σ) respectively are the viscosity, density, and surface tension of the feed droplet; L is a characteristic dimension of the fed droplet (i.e., volume per unit area).

Overall, the literature has succeeded in defining the droplet size of **atomization**, but there are still further steps to consider, such as the **drying** chamber environment and the **collecting** mechanism.

1.4.2. Drying

In the drying chamber of a spray dryer, the process of complete solvent removal, or the transformation of the feed solution into dried granules, occurs according to the

principles of thermodynamics [13]. The main goal of this stage is to expose the droplets to hot gas to facilitate evaporation.

While there are various definitions of evaporation, it can be simplified for the purposes of analyzing the micro-level conditions in a spray dryer, as proposed by Handscomb. In addition to considering the thermodynamics of the drying process, it is also important to consider the chemical potential of the drying gas in relation to the feed solution, as this can have an impact on the drying process. Careful selection of the drying gas and implementation of gas filters or use of specific gases that do not react with the droplets can help to optimize the drying process [14].

In the drying chamber of a spray dryer, the complete removal of solvent from a liquid feed solution is achieved through a process of mass transformation, governed by the principles of thermodynamics. It is important to consider not only the thermodynamics, but also the chemical potential of the drying gas in relation to the feed solution in order to prevent any unwanted reactions. The geometry of the drying chamber is also crucial in ensuring that there is enough space for the particles to be completely dried without sticking to the walls.

A cylindrical chamber with an inverted cone in the base is a common design, although various designs have been developed throughout the history of the spray dryer[14]. The drying process involves heat exchange on the surface of the particles, leading to the evaporation of solvent and the condensation of solute. This is driven by the

difference in vapor pressure between the solvent and the system, resulting in the formation of a dried granules. The drying stages can be described using the model proposed by Handscomb, which involves an initial rapid heating of the droplet followed by a period of constant equilibrium at the evaporation temperature AB at the following figure 6 [15].

Figure 6 shows the timeline of a droplet containing suspended solids during the spray drying process.

Figure 6. Timeline of a spray-dried droplet.[15]

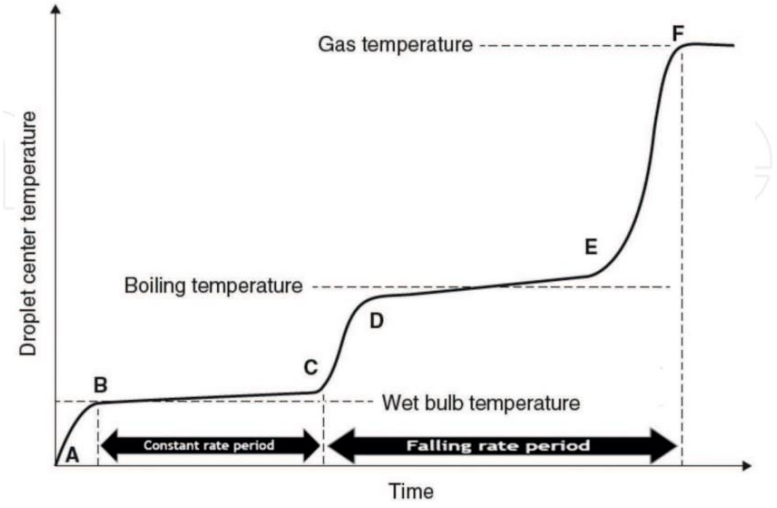

In between BC, Constant evaporation occurs when the surface of the particle is maintained below the wet bulb temperature, which is the gas temperature at the saturation state of a specific liquid vapor. This temperature can also be considered the lowest temperature that the gas can cool to due to evaporation. Cooling and evaporation occur concurrently, resulting in a constant temperature of the particle. This regime of cooling and evaporation from the surface occurs simultaneously as long as there is moisture

supplied from the center of the particle. During this stage of evaporation, a suspended solid forms a shell on the surface of the droplet, and the surface area limits the rate of exchange according to the following mathematical equation.

$$\frac{\partial C}{\partial r} = Pe.C \tag{4}$$

C is the mass concentration of the solid fraction and r is the droplet radius. (Pe) The Péclet number is defined as the dependent unitless value of both velocity of the flow field and a characteristic length L of the system [15]

$$Pe = \frac{vL_{char}}{D} = \frac{K}{D} = \frac{\text{evaporation rate}}{\text{diffusion rate}} \tag{5}$$

A misconnection between the interior particles of the solid within the droplet may form due to a rate-limiting shell, introducing voids inside[16]. At the end, spherical, elongated, pancake-like, or donut-like shapes of granules may be observed. This is explained by the accumulation of solids on the surface increasing the rigidity before the stabilization of the shape.

Konsztowicz has found a relationship between the granule shape and the apparent surface tension and has mentioned the non-understood situation of the thermodynamic principles to explain the effect of the powder particles on the surface tension[14].

During the timeline of droplet evaporation, a decrease in water diffusion rate with an increase in particle temperature occurs at the CD stage. This means that a particle has reached a critical water saturation content after which the kinetics of drying decreases. A critical point is defined for most wet-processed ceramic systems as the point at which particle contact and shrinkage stop [16].

Later in the DE stage, specifically at the boiling point of the solvent, evaporation occurs at a constant rate for the second time during the particle drying timeline. In some cases, an increase in temperature may lead to interior pressure in the particle, resulting in expansion or particle rupture. The end of the drying process can be understood as the point at which there is nothing left to evaporate, and the entire provided heat is consumed by the dry particle, resulting in hot dried particles.

The mentioned timeline of the drying process includes the shape formation of the particle and the rheological behavior of the resulting granules. During drying, there will be a point at which the partial pressure of the moisture vapor inside the particle overcomes the surrounding pressure, which will leave a bubble behind, as shown in Figure 7.

Figure 7. Droplet morphological changes represented during spray drying[6]

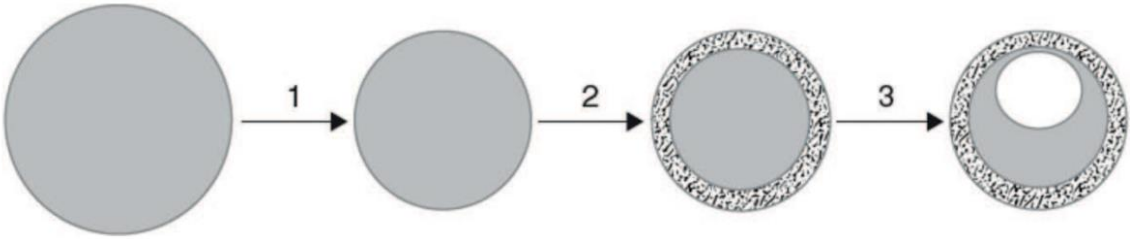

The single most striking observation to have a hollow inside the particle was a result of the following:

- The droplet expands because of the internal energy which is called ballooning.
- The diffusion of solids occurs toward the center of the droplet in the opposite direction of moisture evaporation, evaporation leaves air voids inside the droplet as it happens at a faster rate.
- The slurry's solid ingredient has been attracted to the surface of the droplet during the capillary action of liquid migration.
- Any existing air from the slurry will exist as voids inside.[16]

Further investigations and research reports have studied the final shape of sprayed granules [6, 15]. a simulated model has been proposed to expect the different morphologies of granules results from a spray-dried suspension (figure 8).

Figure 8. Expected morphologies of granules resulted from spray drying[15].

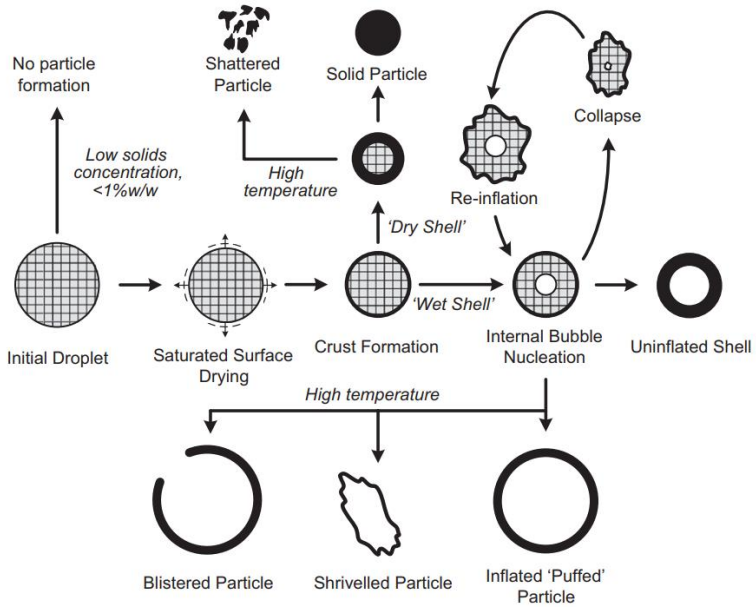

It is clear from the previous figure that many morphologies can be theoretically achieved. While most of them can be produced under one test condition, there are one or two morphologies that dominate during production. In other words, there is no theoretical way to produce a predicted particle morphology. To make a good prediction under the conditions of nucleation, growth, and external parameters, a simulation was proposed by Handscomba[15]. Others showed that by including the central bubble and shell formation in the simulations, a wide range of morphologies can be expected [6, 9, 15].

These results suggest that the droplet size and variety of particle sizes in the suspension allow a specific morphology to form. For example, at a critical solid volume fraction, shell formation is expected to occur, which will have a higher porosity if the included particles from the suspension are of the same size, while a variety of particle sizes gives denser granules. This is called population balance, which is proportional to the prediction of the crust properties to allow bubble growth or continue further drying [15].

Back to history, the following mathematical equation described the control limits of the drying process of a droplet in a spray dryer by calculating the minimum temperature (T_G) that guarantees the full removal of the solvent at the minimum sufficient time (t) that a particle exists in the chamber [13].

$$T_{wb} = K_1 . \left(\frac{T_b}{K_2}\right)^m \log(T_G) + K_3 \quad (4)$$

T_{wb}: wet-bulb temperature
T_b: the boiling temperature
K1 , K2 , K3 and m are Antoine constants.

To calculate the time t.

$$C_m = C_0\,(1 - \frac{t}{\tau_D})^{\frac{3}{2}} \quad (5)$$

C_m: the needed final concentration of the particle after drying.
C_0: the initial concentration.
τ_D: the maximum droplet drying time.

If the evaporation rate is K and we got τ_D from (6) and we know the diameter of the initial droplet, then the maximum droplet drying time can be calculated by:

$$\tau_D = \frac{D_d^2}{K} \quad (6)$$

To conduct a spray drying test, values for the necessary temperature, slurry concentration, and droplet-heat exposure time must be introduced.

1.4.3. Collecting

This is a stage for the collection of dried granules, after mass transformation has occurred via evaporation by an external device. This device typically has a design consisting of an upper cylinder and a bottom conical portion that utilizes centrifugal force and reverses the flow of gas upwards to the exit of the separation chamber, where the separation process takes place [6].

The separation is achieved by separating the particles from the drying gas according to the state of the particle. A dense particle is expected to fall to the conical

portion of the drying chamber and then towards the bottom of the main chamber, while particles that are not completely dried may stick to the walls of the drying/separating chambers or fall to the bottom of the chamber where the flowing gas cannot carry them.

Finally, the flown gas carries the particles to the external separator device. This transportation is dependent on the ability of the gas to carry limited masses to the other side of the machine [7, 14].

The incoming gas to the cylinder design introduces a centrifugal force due to the angled convergence of the exit and entrance of the drying chamber and separator chamber interface, which allows for the free flow of the product [7]. Because of the centrifugal force, the particles are separated from the steam gas. When the gas reaches the cone, it is reversed in the opposite direction due to vortex creation [6, 14]. As a result, the gas exits as a clean gas or is combined with the smallest granules, which are collected by further portable devices if they exist.

Several designs of separating devices have been mentioned in the literature, such as cyclone separators, bag filters, electrostatic precipitators, and venturi wet scrubbers, all of which are used to obtain specific characteristics of the resulting particles [14]. Further explanation about these devices can be found in this study.

Another mechanism for collection involves the use of scrapers. The use of scraper devices becomes necessary when the drying chamber is not equipped with a cone-shaped part or its walls converge at an angle that is too obtuse to allow for the free flow of the product. Scrapers have various designs, such as vibratory devices, mechanical brushes, and a stream of compressed air, but the use of internal scraper devices may cause problems related to the mixing of the dried product with other feed particles that are not completely dried.

To prevent larger particles from falling or to decrease the sticking of undried particles, an additional device can be used to apply hot air by drawing in the exhaust air beside the device supplying hot air into the chamber. This solution is common in spray dryers used at the laboratory scale. Pharmaceutical applications of spray drying often require particles under 10mm in diameter, which creates a need for highly effective external devices for the collection of the dried product.

1.5. Modified designs of spray dryer

The spray drying technique involves three main processes: atomizing, drying, and collecting the product. There have been numerous designs for each of these processes, and the use of various combinations of designs has allowed for a wide range of approaches to spray drying materials such as food powders, medicine drugs, and ceramics. In this section, different designs for atomizers, drying chambers, and collecting chambers will be presented.

1.5.1. Atomizers

The atomization process in spray drying is critical, as it not only drying heat-sensitive materials to produce granules, but also forming droplets with the desired physical, chemical, and morphological properties [7]. The large surface area created through atomization is essential for the evaporation of liquids, as it provides the necessary thermodynamic conditions for this process to occur. For example, one cubic meter of liquid matter can be atomized into droplets with a medium size of 100 μm, resulting in a surface area of 60,000 m^2 [7].

There are several ways to classify atomizers based on various characteristics. These include the type of energy used for atomization, such as pressure, kinetic, centrifugal, sonic, or electrical energy, and the size of the spray dryer. Atomizers can also be classified based on their relationship to pressure, atomizer speed of rotation, or atomizer diameter, as well as their ability to feed a certain amount (in mL/min or L/h) of material without clogging. Additionally, atomizers can be defined by their capacity to produce a series of linked atomized droplets [6, 7].

The most conventional types of atomizers are rotary nozzle, two-fluid nozzle, pressure (hydraulic) nozzle, ultrasonic atomizer, and electrohydrodynamic nozzle.

Rotary atomizer

A horizontally positioned wheel or disc is used to feed the slurry at the center. An external motor applies a centrifugal force, causing the supplied feed to be accelerated

towards the perimeter of the disc. Where droplet formation occurs beyond the perimeter (figure 9).

Figure 9. Rotary atomizer

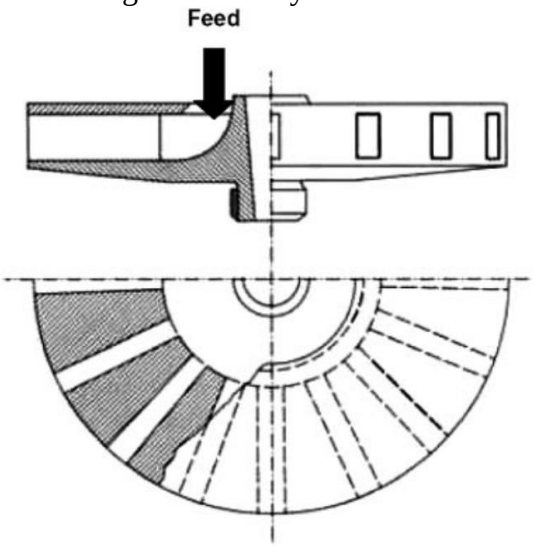

The design of the grooves and the speed of rotation contribute to the controllability of solution dispersion. Curved grooves can increase the density of the resulting granules, while straight grooves with non-grooved regions can improve the flowability of the granules. However, the rotary atomizer has the drawback of depositing many droplets on the walls of the drying chamber [7].

Pressure (hydraulic) nozzle

The one-fluid nozzle, also known as a hydraulic nozzle, works by conducting the feed under pressure through a pipe with a decreasing diameter (figure 10). This is illustrated in Figure 10. The last opening of the pipe has a diameter range of 0.4 to 4 mm, and the atomization angle is typically in the range of 40-160°.

Figure 10. Schematic representation of a hydraulic nozzle[7]

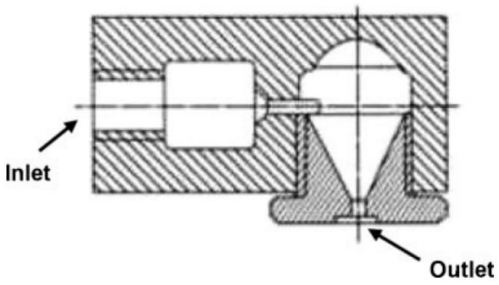

However, this type of nozzle has limitations in terms of the materials it can handle. Hard materials may cause abrasion in the nozzle, and it is not suitable for high-viscosity solutions. In low viscosity solutions, clogging is a common issue.

Pneumatic (Two-fluid) nozzle

The multi-fluid nozzle, commonly known as a two-fluid nozzle, involves the use of two fluids: the feed solution (such as a slurry in ceramics) and the atomizing pressured air. Both fluids follow their own path towards the end of the nozzle, where they meet at the central collision point. This point can be located inside the nozzle or outside, depending on the operator's preference. The high velocity of the gas impacts the liquid surfaces, creating frictional forces that generate droplets.

Figure 11. Two-fluid nozzle[7]

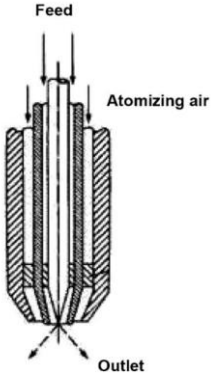

Generated droplets and resulting granules are affected by:

- Gas velocity
- feed density
- gas/solution outlet ratio
- solution surface tension
- feeding direction

To prevent clogging, a needle controlled by compressed air is positioned in the nozzle. This needle helps to supply the feed and clean the nozzle, but it also restricts the area from which the feed is supplied. This can result in heating the solution (such as a slurry) before atomization. There are other nozzle types that can be used for high-viscosity solutions, such as ultrasonic nozzles and electrohydrodynamic nozzles, but they are not relevant to this study.

1.5.2. Drying chambers

The design of the drying chamber plays a crucial role in achieving two important results: the production of fully dried particles with complete moisture removal. The drying chamber is typically a vertical vessel with a cylindrical body and an inverted conical bottom design. In the past, attempts were made to simulate the function of a horizontal drying chamber, but these were ultimately unsuccessful and only reached the stage of computer simulation [17]. Drying chambers are classified into tall and small ones, with the tall drying chamber having a 5:1 ratio of height to diameter, and the small drying chamber having a 2:1 ratio. According to KRZYSZTOF, small drying chambers tend to

have relatively high functionality when used with disc atomizers and nozzles [7]. The size of the drying chamber is chosen based on the desired characteristics of the production and the application field being investigated [7, 14].

The shape and dimensions of the drying chamber are important because they influence the time that the droplets spend drying along the axis of the chamber, which has a corresponding temperature profile [7, 14]. Care must be taken to ensure that the drying chamber design provides sufficient time for the largest expected droplets to dry. However, small droplets (less than 5 μm) tend to dry instantly during the early stages of the hot gas-droplet contact step [7].

Calculations are typically used to determine the appropriate values for the drying chamber, but the complexity of the hydrodynamics and interactions between the two phases involved can lead to frequent calculation errors. As a result, approximation and testing are often used to determine the required size of the drying chamber.

During the drying process, it is possible to control the small variations in the resulting morphology of the final product by ensuring uniform gas flow throughout the volume of the drying chamber and using an air disperser that has a significant effect on this situation, along with the chamber design [6].

Finally, the drying chamber can also be classified based on the positions of the inlets and outlets, which divide the drying chambers into co-current, counter-current, and mixed flow chambers. Figure 12 illustrates these three designs.[7].

Figure 12. Drying chambers of spray dryer (a)Co-current (b)Counter-current (c)Mixed mode[18]

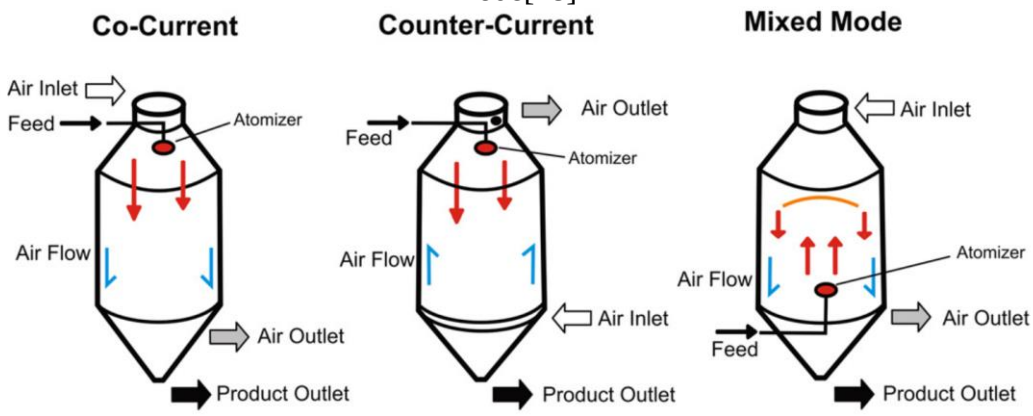

(a) (b) (c)

Co-currently chamber

In the co-current drying chamber design, the inlet airstream and atomizing spray are positioned at the top of the drying chamber. As the particles fall within the chamber, they lose their liquid content [7, 14].

Since the feed and hot air are supplied from the same upper position, the drying gas does not have time to exchange heat with the surrounding environment. As a result, the droplets encounter a temperature gradient, with the highest temperature at the top and decreasing towards the bottom of the chamber. A high number of undried particles may not have enough time to dry before hitting the walls and sticking there [14].

This design uses two sources of air: the atomizing pressured air and laminar air streams from a fan. The heat, atomization, and air pressure of this system are uniform, leading to a slow drying process [7]. The dried particles are collected at the bottom through an outlet along with the airflow.

Counter current chamber

In the counter-current drying chamber design, the inlet airstream is supplied from the bottom, and the atomizing spray is placed at the top of the drying chamber. The applied hot air loses much of its heat before coming into contact with the droplets. The droplets undergo a drying process that ends at the hottest air zone.

The outlet has a lower temperature than the products in this design. The products contain pores that are introduced because the droplets are further heated to ensure complete drying. Powders with low heat resistance may not be suitable for this design. The particles are collected from the bottom, and the outlet air exits from the upper part.

Mixed flow chamber

The mixed flow drying chamber design combines elements of the co-current and counter-current designs. The atomizing spray is placed at the bottom of the chamber, while the inlet airstream is supplied from the top. The path of the droplets is reversed due to the counter-current position of the atomizer relative to the inlet drying air. This design produces a moist product with dried products mixed in the collection bottle. The dried particles and outlet air flow are released together at the bottom of the drying chamber.

1.5.3. Collecting devices

As previously mentioned, there are primary and secondary separation stages that take place at different positions in the machine. One occurs at the bottom conical shape

of the drying chamber, while the other involves the discharge of evaporated moisture and granule particles through a conveyor/pneumatic system [6].

The primary separation stage begins at the bottom of the drying chamber. It can be facilitated by additional scraper devices if the chamber design is not cone-shaped at the bottom, or if the walls converge at too obtuse an angle for product flow. In some cases, an additional assembled separator is used as a secondary assistant separator. However, using scraper devices can lead to problems related to the purity of dried products, as the feed suspension may not be completely dried. The most common scraper devices used are vibratory devices, mechanical brushes, and a stream of compressed air [6, 7].

Operators have the option to design their separation system, but there are three mandatory options: a cyclone separator, a bag filter, and an electrostatic precipitator [6]. The following sections provide information on the various designs of cyclone separators.

Cyclone separator

The cyclone separator is the most commonly used separator for spray drying. It consists of a cylindrical upper part and a conical bottom part, resembling a cone. In a cyclone separator, the solid granules are separated from the air using centrifugal force caused by a spiral vortex. This force causes the granules to flow around the walls and move downward. At the same time, the spiral vortex carries out very fine particles. The gas reaches the end of the cone, where the vortex is created in the opposite direction. Large particles/granules are directed downward and are not affected by the vortex [6].

Figure 13. Cyclone separator[14]

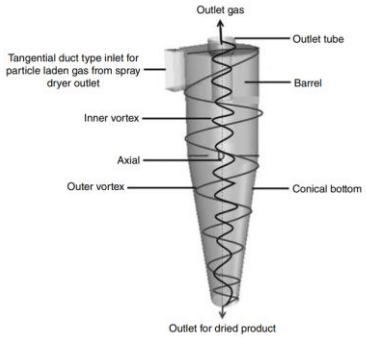

Bag filter

Bag filters are columns of metal that contain fabric bags. granules enter the filters with an airflow and stick to the fabric surface. The fabric has pores with a variety of diameters, which increases the efficiency of granule collection. The granules are then discharged through various mechanisms.

Figure 14. Bag filters[14]

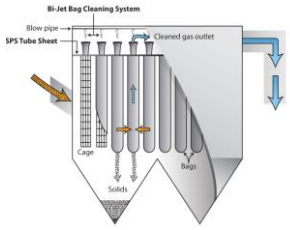

Electrostatic precipitator

An electrostatic precipitator uses an electrostatic force to collect particles after spray drying. By applying a high voltage to the discharging wires, the air around is ionized to supply ions. According to Coulomb's forces, the charged particles converge to the collecting plates.

Figure 15. Electrostatic precipitator[19]

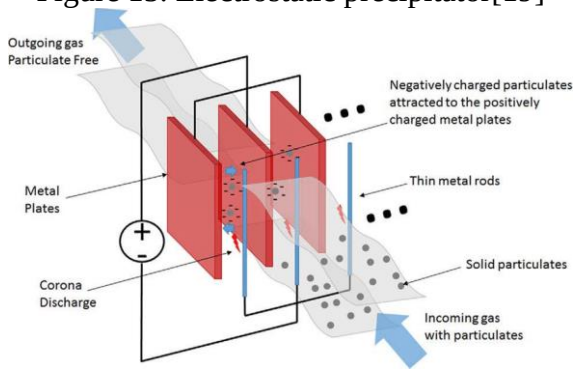

1.6. Effective parameters of spray dryer

Much of the research conducted has focused on the effect of slurry composition on the final granule shape and properties [5, 16, 20-24], while the influence of spray dryer parameters on the production of alumina granules has not been extensively studied. Many other general factors that influence the physical properties of the produced granules have been mentioned [7, 14]. The effects of drying temperature, feeding rate, atomizing air pressure/quantity, droplet size, and outlet temperature have been investigated as machine parameters of the spray drying process [11, 12, 25].

Operating a spray dryer can be complex, and the operator can have as much influence on the granules as the sprayed material characteristics. The machine parameters are adjustable for each material and can be optimized based on the feeding dispersion composition and desired final granules.

It is important to understand that the effects of spray drying foods do not necessarily apply to ceramic drying. However, there are generally reliable assumptions

for manipulating machine parameters. For example, at a constant air inlet pressure, the granule size can be adjusted by the solid content of the slurry [7, 23].

1.6.1. machine parameters:

The schematic in Figure 16 illustrates the effects of five different parameters on outlet temperature, particle size, final moisture content, and efficiency.

Figure 16. Spray dryer parameters and their effect on resulted granules

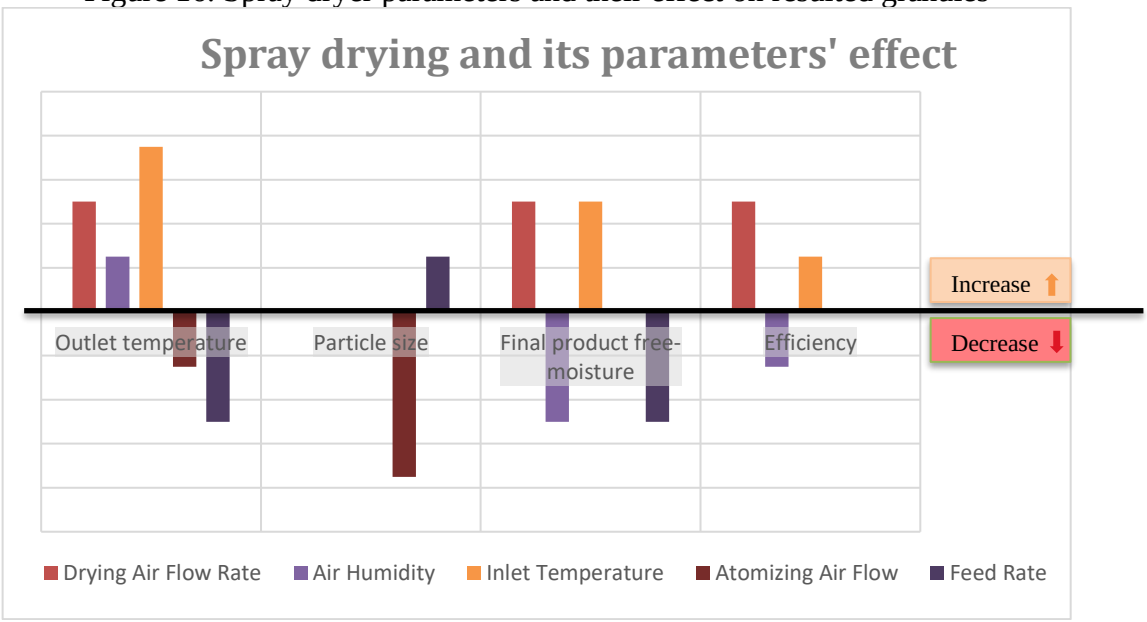

Increasing the drying air flow rate will increase the outlet temperature as there is less heat loss relative to the total energy. However, this will also result in a higher moisture content in the final product as the vapor partial pressure decreases. The efficiency of separation in the cyclone may also get improved [7]. Increasing the humidity of the system will consume more energy to remove moisture and may also result in

particles with higher moisture content. This can negatively impact the outlet temperature and reduce the efficiency of collecting granules [7].

Increasing the inlet temperature will also increase the outlet temperature and decrease the moisture content of the product. This can improve the efficiency of the process, but it is important to note that there is a limit to the temperature that can be used [7]. Increasing the atomizing air flow will decrease the outlet temperature as there is more air to be heated. However, it may also result in larger particle size as the energy of atomization increases [7].

A higher feeding rate will consume more heat for evaporation, resulting in a lower outlet temperature. It will also produce larger particles as there is more liquid for the solid content to disperse in. However, this may also result in incompletely dried particles, which can be either a disadvantage or an advantage depending on the application [7].

1.7. The slurry of ceramic for the spray drying technique

Ceramic materials are typically formed into granules through the use of the spray drying technique. However, errors in this process can lead to the formation of irregular particles [16]. The shape of the resulting granules is influenced by factors such as the initial separation of droplets from the slurry, the evaporation rate, and oscillations during the process[26].. Possible morphologies for ceramic granules include elongated, pancake- or donut-shaped particles, as well as needle-like shapes that may be formed when a rigid surface layer forms before atomization occurs [27].

The initial particle size of the powder used also impacts the resulting granules [28]. The particle size distribution influences the formation of the shell of the granules and the limits of the capillary forces within the granule void, which in turn affects the packing density and crushability of the granules [29]. The packing density of granulation can range from 6% to 65%, although ideal spherical particles can achieve a packing density of 74% [30].

Studies have shown that using initial particles with a D50 of 0.25, 0.8, and 6 μm in the spray drying process resulted in granules with the largest size for the 6 μm particles [31]. The ball milling machine is often used to crush the particles of the received powders.

While the morphology of the granules has been the focus of much investigation, studies on the effects of the initial solid content on granule morphology have also been conducted [8, 10-12]. These studies aim to examine the qualitative and quantitative selection of binders and dispersion agents, or the dispersion state without the use of a deflocculant. The role of these ingredients will be discussed in further detail in this section.

1.7.1. Binders

Binders are organic polymers with functional groups such as acrylics, vinyls, and ethylene oxides that have either hydrophobic or hydrophilic properties [10, 32]. The most

commonly used binders for ceramic powder spray drying are polyvinyl alcohol (PVA) and polyethylene glycol (PEG) [5, 10, 23, 32-34]. Several studies have shown that the solid content in the slurry, which includes deflocculant and binders, influences the spray drying process and should be between 30-40% of the mass of the slurry to achieve granules with a well-stabilized spherical shape [8, 11, 12, 16, 35]. The type, amount, and method of adding the binder to the slurry are also important factors that have been well documented in the literature [16, 24, 32, 35]..

Binders are necessary for creating an interconnect network connection between primary particles in the dried granules during green body production. They provide chemical or physical bonds between particles, so the choice of binder material depends on the bulk material and the required chain length. It may be necessary to use more than one binder to improve the compressibility, bulk cohesion, and plasticity behavior of the powder, which will be reflected in the properties of the sintered body [10, 32]. During sintering at elevated temperatures, the binders will burn up.

Another important consideration when selecting a binder for spray drying is the glass temperature (T_g) of the organic polymer. The T_g is the temperature at which the material transitions from a rigid state to a viscous, rubbery state occur. Using spray drying at temperatures above the T_g can be problematic because it can increase the stickiness of the product on the walls of the chamber. The Gordon-Taylor equation, which considers the solutes present in the slurry, can be used to calculate the optimal temperature for the process. This equation explains the glass temperature of multi-component systems.

$$T_g = \frac{w_1 T_{g1} + c w_2 T_{g2}}{w_1 + c w_2} \quad (7)$$

w_1, w_2 are solute and water mass fractions
T_{g1}, T_{g2} are solute and water glass temperatures in kelvin
C is the ratio of specific heat change of solute to water.

The addition of a binder can increase the viscosity of the slurry, and using a different type of binder can result in different viscosity behavior. In one study, the organic binders used were polyvinyl alcohol (PVA), polyethylene glycol (PEG), and derivatives of carboxymethyl cellulose (CMC), with no dispersant included. It was found that PVA and PEG resulted in the lowest viscosity, while the hardest grains were produced using CMC [23].

In terms of green density, PEG had a higher value compared to the high green density of the body containing PVA. However, when tensile strength was compared for the two green compacts, the body with a higher green density containing PVA had a higher tensile strength. To improve compacts containing PEG, it was suggested to add hydroxyethyl cellulose as a co-binder.[23].

1.7.2. Lubricants

In the literature, polyethylene glycol (PEG) is mentioned as being used as a lubricant during spray drying. The main functions of lubricants are to:

- Help in the separation of the green body from the pressing die, with no sticking of the particles on the walls.
- Add to the interconnect network connection between primary particles at the green body.
- Burn earlier than lubricant during sintering. that opens ventilation voids for binders later during the sintering process.

1.7.3. deflocculation

Deflocculation or dispersion both refer to the process of creating a homogenous, well-mixed slurry of solid ceramics. Highly deflocculated slurries result in granules that can pack particularly tightly and achieve higher densities [16].

1.7.3.1. Why deflocculation?

Deflocculation is an important process in spray drying, as it helps to prevent the agglomeration of particles that can occur due to van der Waals attractive forces. Agglomeration can lead to a range of viscosity values in the slurry and make the spray drying process more difficult, potentially affecting the properties of the resulting granules [23, 35]. To prevent or eliminate agglomeration, it is necessary to break the attractive forces between particles and disperse the solids in the slurry using repulsive forces such as electrostatics or steric effects, or both. This can be achieved by studying the zeta potential behavior of the ceramics at different pH values and selecting an appropriate dispersion agent [23].

The level of deflocculant in the slurry can also influence the density of the resulting granules. Higher levels of deflocculant give the particles a larger mean free path

in the suspension, leading to higher-density granules after water is removed. However, lower levels of deflocculant increase the likelihood of agglomeration, which decreases the mobility of the particles and hinders their rearrangement during water removal, resulting in lower-density, non-uniform granules [16].

1.7.3.2. What is the mechanism of dispersion?

Dispersion is the process of preventing the agglomeration of particles by using repulsive forces. Electrosteric dispersion involves the use of both electrostatic and osmotic pressure repulsion to separate particles. Electrostatic repulsion occurs when charged sides of polymer groups repel each other, while osmotic pressure repulsion occurs when the overlap of adsorbed layers of polymer is resisted. Uncharged polymers can be adsorbed on electrostatically charged surfaces, or charged polymers derived from polyelectrolytes can be used. According to the graph below, using both electrostatic and steric repulsion potentials has a stronger effect in dispersing solid particles than using only Van der Waals attractive potential [35].

Figure 17. Interaction potential according to the dominant mechanism of repulsion between particles[35]

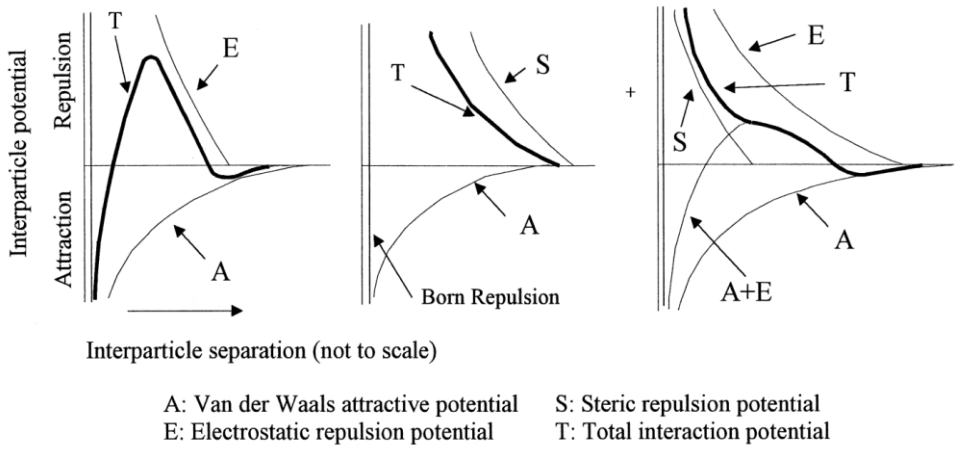

Certainly. The way in which a polymer adheres to the surface of particles in a suspension can be influenced by the zeta potential behavior of the material being used and the charge or uncharged state of the dispersion agent polymer. In Figure 18, it is shown that polymers can adhere to the surface of particles in three different configurations: train, loop, and tail. These configurations are determined by the pH of the medium in which the solid is suspended. Polyelectrolytes, which are polymers that have both a hydrocarbon chain and a polar ionic part (such as COO^- or $SO3^-$), tend to produce a tail configuration when adsorbed on the surface of particles. This configuration pushes the particles away from each other, reducing the likelihood of agglomeration [23, 36]. The figure below illustrates the ceramic powder surface in suspension with train, loop, and tail configurations [35].

Figure 18. Ceramic powder surface in suspension represented with train, loop, and tail configurations[35]

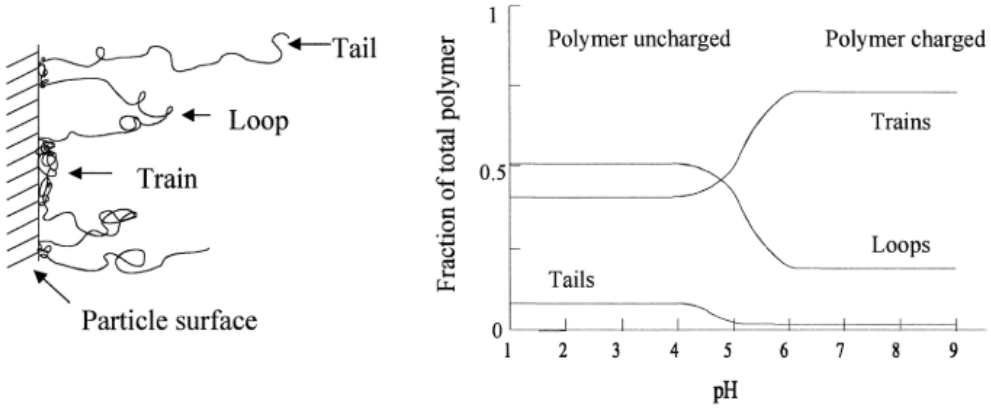

Additionally, it is important to understand the concept of the electrical double layer in order to understand the properties of the alumina being used and the amount of dispersant required. When a ceramic particle has a positive or negative charge on its

surface, it will attract opposite ions from the bulk solution near the surface of the particle, creating a layer known as the shear or slipping layer. Furthermore, a diffuse layer is formed at a distance from the particle where more ions of the opposite charge are attracted to the particle from the bulk solution. This layer also contains a small amount of charges of the same sign as the particle.

The electrical double layer that is formed has a specific potential, which is a measure of the energy required to bring a unit charge from a group of hundreds of charges with the same sign, taking into account the repulsion between them. This electrical potential energy has a unit of voltage. The potential is a measure of the repulsion that will exist between particles based on their separation distance. In this case, the potential is a characteristic of the material or medium known as the zeta potential. The figure below illustrates this situation visually (figure 19).

Figure 19. (A) Zeta potential on a graph of electrical potential and distance between particles (B) Electrical double layer[37]

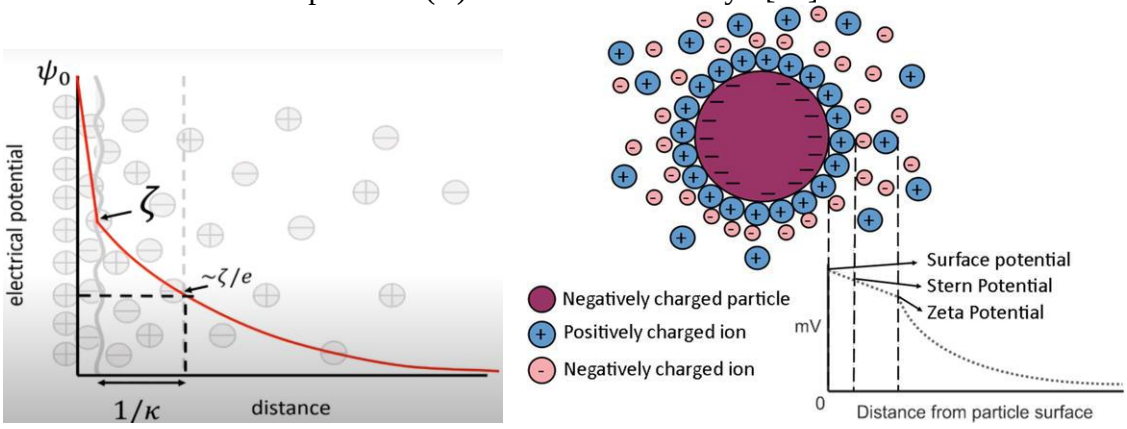

(A) (B)

Zeta potential is a potential that describes the surface charge of a solid in contact with a liquid, typically water. It is the potential on the slipping plane and decreases beyond the diffuse layer due to the electrolyte and polar nature of the liquid. The effective range of the zeta potential of a particle can be controlled by changing the concentrations of ions in the bulk solution. In Figure 20 (B), a thick double layer is shown, while in Figure 20 (C), a very thin double layer is present due to the high concentration of ions collected on the diffuse layer. However, ions are still exchanged between the particle and the bulk solution within the diffuse layer.

Figure 20. The effect of different electrolyte concentrations on the thickness of EDL concentration increases from (A) to (D) respectively.[37]

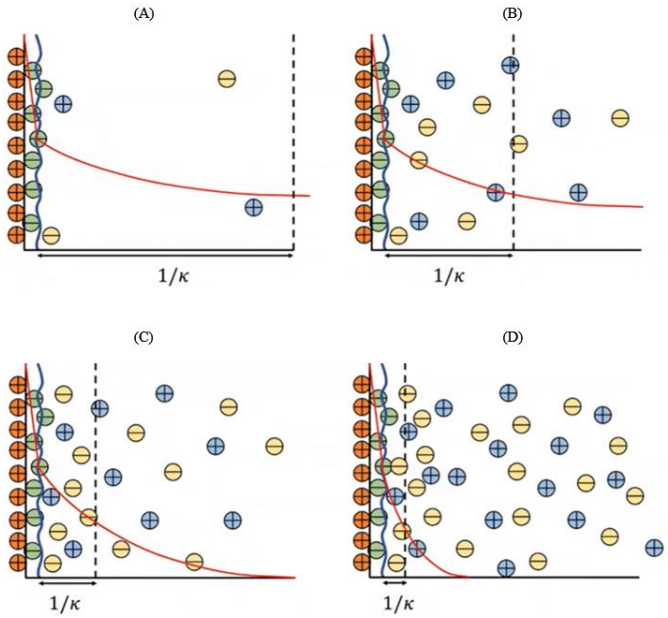

Increasing the ionic strength of the solution also leads to a thinner double layer. When the electrical double layer (EDL) is very thin, it is said to be collapsed. Ionic strength is a measure of the concentration of all ionic species present in the solution, taking into account their valences. The opposite situation, where the highest ionic

concentration has no barrier to particle agglomeration, is described as an aggregation energy barrier.

Figure 21. Total repulsion/attraction forces of the cases in figure 20.

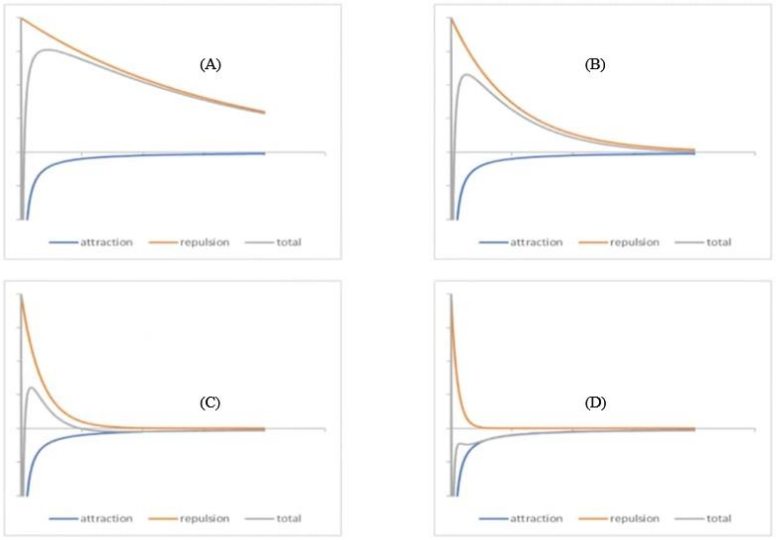

To adjust dispersion, it is necessary to alter the size and optical properties of a particle, as the zeta potential cannot be changed otherwise. On the other hand, the thickness of the electrical double layer (EDL) can be controlled through the selection of electrolyte concentrations and the addition of an ionic surfactant.

1.7.3.3. Deflocculants in literature

There have been numerous efforts to achieve high dispersion in a slurry of alumina particles for spray drying. Cesarano et al. found that the charge of alumina particles in suspension depends on the pH, with a point of zero charge at around pH 8.7. They also discovered that the molecular weight of the polymer used can significantly affect the stability of the slurry when added to high solid levels [38].

Tjipangandjara used fluorescence spectroscopy to study the effect of adding a specific amount of polyacrylic acid (20 ppm, 88,000 molecular weight) on the zeta potential of the alumina particles and found that it changed the zeta potential over a smaller pH range above 7 [39]. Another study reported that using polyacrylic acid as a dispersant can stretch the polyelectrolyte chains on the surface of the particles due to the repulsion between negative carboxylic groups [5].

Low slurry viscosity at a shear rate of 50 s^{-1} (0.017 Pa.s) has been reported for a 77 wt.% solid load using 0.4 wt.% of a carbonic acid-based polyelectrolyte dispersant at room temperature [21]. In a separate experiment, Samir Baklouti worked with a 60 wt.% solid load dispersed using 0.16% polymethacrylate salt with a molecular weight of 10,000. The binder amount used in this experiment was between 1-3 wt% relative to the solid load, and polymers of polyvinyl alcohol (31,000 molecular weight) or polyethylene glycol (20,000 molecular weight) were employed. The spray drying was carried out using pilot plant equipment [40].

1.8. Slurry parameters

The preparation of a slurry containing alumina in water involves mixing alumina powder with water to form a suspension of ceramic particles in water. The process can be done both physically and chemically. Physically, the alumina powder can be mixed with water using mechanical means such as a stirrer or a blender. This process will result in a suspension of alumina particles in water, but the particles will not be fully dispersed and may have a tendency to settle over time.

Chemically, the alumina powder can be dispersed in water by adding a dispersant, which is a substance that helps to keep the ceramic particles in suspension. The most common dispersant used for alumina is polyacrylic acid (PAA), which forms a complex with the alumina particles and reduces the surface energy of the particles, allowing them to be more easily dispersed in water.

The interactions between binders and dispersants have a direct impact on the behavior of the suspension during spray drying, which ultimately affects the quality of the produced granules. Dispersion is critical for ensuring that the solid particles are well-mixed and evenly distributed in the slurry, as well as for controlling the viscosity of the slurry after the addition of solids, binders, and deflocculants. During spray drying, the suspension is fed through a silicon pipe at a controlled rate and into the nozzle tube. Calculations are used to determine the optimal viscosity for the slurry to flow smoothly through the nozzle or pipe.

In a pneumatic system, the shear rate just before the nozzle end is approximately 10^4 s^{-1}, which increases to 10^6 s^{-1} upon contact with the airflow. It is also important to consider that temperature changes can affect viscosity, and shear thinning may occur during the feeding process. In these situations, it can be helpful to use the Casson equation for viscosity calculations [41].

$$\tau^{0.5} = \tau_Y^{0.5} + \eta_\infty^{0.5}\gamma^{0.5} \quad (8)$$

τ is the shear stress. γ is the shear rate. τ_Y is the yield stress. η_∞ is a viscosity limit for an infinite shear rate

In theory, attractive forces between particles in a slurry can lead to the formation of weakly bonded networks of particles known as flocs. If there are many flocs present, the resulting structure may require a certain amount of yield stress, or resistance to flow, in order to flow freely. This yield stress (τ_Y) can break down the flocs at higher values, and the viscosity of the slurry may reach its limit for an infinite shear rate (η_∞) at this point [16].

An increase in electro-steric dispersion can add to the yield stress value, which can decrease the density of the granules by decreasing the mobility of the particles during drying. Both the binder and solid load can have a significant effect on the infinite viscosity ($\eta\infty$). According to Krieger [42], the viscosity of the suspension is proportional to the volume fraction of solids in the slurry. Additionally, an increase in electrostatic dispersion can add to the yield stress value, which can also decrease the density of the granules by decreasing the mobility of the particles during drying.

$$\frac{\eta}{\eta_0} = \left(1 - \frac{\emptyset}{\emptyset_0}\right)^{-[\eta]\emptyset_0} \quad (9)$$

η is the suspension viscosity
η_0 the viscosity of the pure solvent liquid
$\emptyset$ is the solid volume fraction
$\emptyset_0$ is the solid critical loading where η goes to infinity according to equation 8.
$[\eta]$ is the intrinsic viscosity, a factor for the particle shape behavior hydrodynamically.

Using an organic solvent instead of water in spray drying can lead to an increase in outlet temperature, because the energy required for evaporation is lower. As a result, the particles produced tend to be larger due to the lower surface tension. One of the biggest advantages of using an organic solvent is the ability to achieve a very dry product.

However, it is important to consider that the efficiency of the overall process may become dominant [7].

Figure 22. Slurry ingredient parameters and their effect on resulted granules and efficiency of the machine

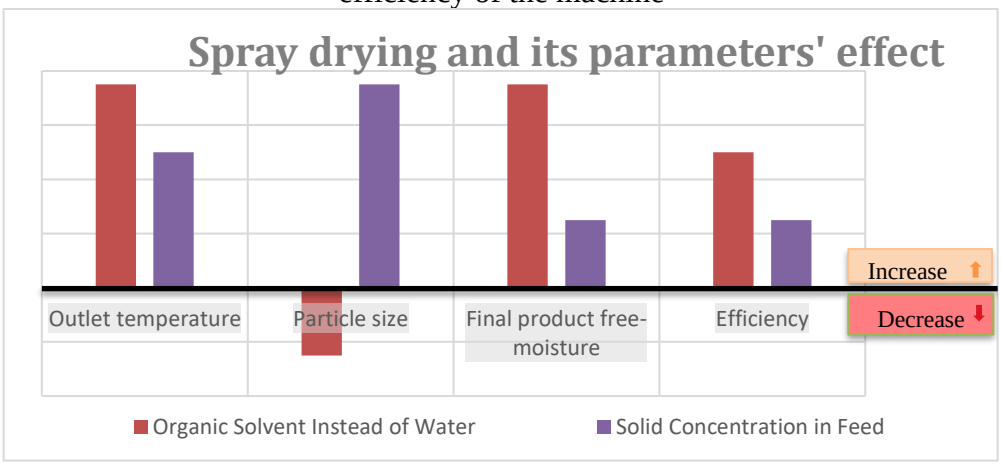

Using a higher solid concentration in the feed for spray drying will reduce the amount of water that needs to be evaporated, leading to a higher outlet temperature. This can also result in an increase in particle size, as the higher solid content leads to larger particles. Additionally, the moisture content may be lower due to the lower partial pressure. The efficiency of the process may also improve, as larger particles can be more easily collected through the cyclone separator [7].

1.9. Slurry for Alumina granules in literature

1.1.1. Studies on granules of Alumina

Studies on the properties of alumina and its granules have highlighted the importance of this material and shown the role that its preparation and ceramic processing

can play in its characteristics. For example, Hotta found that using methylcellulose as an organic binder in a granule layer manufacturing process led to improvements in the green body density and sintering of alumina [43].

Other studies have examined the relationship between binder content and the properties of sintered bodies, finding that binders such as PEG and PVA at a content of 3 wt.% in the green density of alumina sintered at 1600°C resulted in high tensile values of 129 MPa [34]. TAKTAK also explored the use of PEG or PVA as binders during spray drying of alumina powders and their impact on the mechanical strength of the sintered body [44]. In [32], it was observed that the sintered density of compacts made from powders containing higher amounts of PEG was lower than those containing lower amounts of PEG.

In addition, the procurement of raw material for nano alumina powder has been shown to benefit from granulation through spray drying under specific slurry conditions (2 vol% alumina, 6 wt% PEG, 0.02 wt% sodium hexametaphosphate), resulting in a suitable powder for plasma spraying techniques [45]. Previous research has also indicated that the morphology of alumina has a direct effect on the compaction behavior and flexural strength of alumina bars [46]. Ghanizadeh found that spray-freeze drying primary alumina fine particles of approximately 150 nm led to better flowability and crushability, resulting in green densities of over 50% of the theoretical density [47].

The morphology of alumina granules and its impact on the mechanical properties of sintered alumina has also been the focus of Reed, who noted that spheroidal granules with lower density and low apparent yield pressure resulted in higher density sintered bodies than those using spheroidal or hollow granules with higher apparent yield pressure and higher density [22]. Reed also discussed the common problem of craters in ceramic granules and their formation, which can occur due to factors such as increased binder content, higher binder molecular weight, high air temperature, or decreased solid loading. These craters, also known as blowholes, can result in a thinner crust, which is more prone to collapsing when exposed to low heat and a slower drying rate [15].

Another study found that the addition of organic binders to spray-dried powders can increase Young's modulus of the green body [48]. The optimization of spray drying techniques requires an understanding of the feed material and its powder, as well as an examination of the influence of machine parameters on the morphology and optical properties of the resulting granules [8].

The addition of lubricants, such as PEG with molecular weights of 20M and 8000, has also been studied, with the compound containing 20M PEG found to adsorb onto the surface of the alumina more readily than the compound containing PEG-8000 [49]. Granules resulting from the more adsorbed PEG compounds (20M PEG) were found to have lower densities than those made with PEG-8000-containing compounds [16]. Overall, researchers have investigated the effects of slurry on the morphology, flowability, and mechanical properties of granules, as well as the impact of various machine parameters.

1.1.2. Summary

The following table has a summary of the used materials in the slurry content, besides the method of spraying for alumina granules, according to the latest literature review (table 2).

Table 2. Spray drying of alumina in the history with the given values of the parameters.

Ref.	Compound parameters			Machine parameters				Resulted granule	
	ceramic	binders / Lubricants	deflocculant	PH	in ℃	out℃	pressure	size	notes
[47]	α-alumina			-	210	120		70-90 µm	sprayed using a rotary atomizer or a probe operating 230 KHz. Slurry stirring is done by an ultrasonic device
[46]	Alumina 77 wt.%	4%		8.3	260	115	5 psi	47 µm	
	Alumina 77 wt.%	4%		8.3	250	110	4 psi	55 µm	
	Alumina 82 w.t%	4%		8.3	250	113	5 psi	36 µm	
[50]	50wt% pure α-alumina and yttria (3 mol %) stabilized zirconia	1,3 wt % PEG 4000		6.5	180	85		50-70 µm	ultrasonic spray dryer 20 Khz
[10]	(99.9%) gamma alumina nanopowder 35 vol.%		polyacrylic acids with H+ or Na+ side groups (PAA or PAAS) 2100,2000,5000,15000 Molecular weight	9 to 11	160±5	85-90		80 µm	20 kHz ultrasonic stirring. The viscosity of the slurry was 0.40 to 0.51 mg/m2

Ref.	Compound parameters			Machine parameters				Resulted granule	
	ceramic	binders / Lubricants	deflocculant	PH	in ℃	out℃	pressure	size	notes
[22]	80 gram of Al2O3 over 150 total soln	PVA and PEG			220	120			ultrasonic of 20 kHz for stirring
[9]	30 or 40 vol% powder Reactive-grade alumina	3.0 wt% PEG Compound 20M	0.35 or 0.75 wt% deflocculant PAA with a molecular weight of 6000		200	95-105		50-100 µm	mixed-flows spray dryer with a pneumatic atomizer/co-current spray dryer using a wheel-type atomizer.
[12]	35 vol% alumina slurry,	1.5 wt% binder PVA 4% lubricant stearic acid	0.5 wt% dispersant PAA		100	65	8-10 kPa	25-45 µm	
[26]	70-80% alpha Alumina	2% CMC PVA PEG PAE						5-50 µm	CMC gives high viscosity, a uniform size distribution
[8]	alpha alumina 30 vol% means 50 wt%	PVA 4wt% and acrylic ester	The ammonium salt of PAA (PAANH4), an average molecular weight of 7000 to 8000 concentration of 0.04 wt.%	> 7	220	140		5-50µm	
[24]	(77 wt.%) α-alumina powder	Dolapix (CE64) in 0.3-0.5 wt.%							

Ref.	Compound parameters			Machine parameters				Resulted granule	
	ceramic	binders / Lubricants	deflocculant	PH	in ℃	out℃	pressure	size	notes
[40]	60 wt% alumina	partially hydrolyzed (88 mol%) PVA (4-88, MW=31 000,	0.16 wt% of PAA salt (PMAANH4 +, MW=10 000)					200μm	spray-dried in pilot plant equipment.
[40]	60 wt% alumina	(PEG 20M, MW=20 000,3 wt% for PEG and 1 or 3 wt% for PVA.	0.16 wt% of PAA salt (PMAANH4 +, MW=10 000)					200μm	spray-dried in pilot plant equipment.
[9]	alpha-alumina	PEG	silicon nitride and poly(vinyl butyral) (PVB)						Hollow granules form when a high dispersant level is used. particle packing density in solid granules is lower than in hollow granules.
[45]	Alumina 22 vol%	PEG 6 wt.%	Sodium hexametaphosphate 0.02 wt.%		300	100	N2 gas 0.9–1.2 bar		

1.10. The objective of this study.

After reviewing the literature, it seems that many studies do not provide specific values for flowability and instead simply describe their granules as flowable within a size range of 15-70 microns. Additionally, some studies have examined various types of spray dryers, with co-current systems being the least commonly used for ceramics. It is also important to note that machine parameters can vary significantly between different designs.[5-8, 10-14, 16, 17, 20, 23, 26-31, 43, 45-47, 50-52].

There appears to be a lack of information on how the properties of granules are affected by changing spray dryer parameters, as well as how changes in the solid load in the slurry may impact the granules and where to collect particles from the machine. This study aims to understand the relationships between these variables and their impact on granules properties like:

- Flowability
- Particle size
- Crushability
- Green density
- Sintered density

2. Experimental method

2.1. Materials

A commercial powder of Alumina (Al_2O_3) Eti-Fine 706 (Eti Aluminyum, Seydişehir, Turkey) was used as the initial material. Alumina was calcined at 1200 ℃ to have α-alumina.

The binders and lubricants used in this study were

- Polyvinyl Alcohol (PVA) Bp17 (ZAG, Istanbul, Turkey)
- Polyvinyl Alcohol (PVA) 363170 (Sigma-Aldrich, Darmstadt, Germany) 13000-23000 M.
- Polyethylene Glycol PEG-400, 1500, 4000 (Labshop41, Istanbul, Turkey)
- Polyethylene Glycol PEG 6000 (8.07491.1000Sigma-Aldrich, Darmstadt, Germany)
- Sodium nitrate $NaNO_3$

2.1.1. Particle size analysis.

The particle size of the received powders was analyzed by dispersing 50 mg of the powders in distilled water. The Mastersizer 3000 laser diffraction particle size analyzer, manufactured by Malvern in the United Kingdom, was used to measure the particle size distribution. This device consists of a main optical source (a laser) and a

dispersion unit that circulates the slurry through the optical pass towards the detector. The range of particle sizes that can be measured by this device is from 100 nm to 2 mm.

2.1.2. Microstructure analysis of powders.

The microstructural analysis was imaged using a Leo Supra 35 VP FEG SEM from Zeiss in Oberkochen, Germany. This was done to observe the differences in the morphology between the received powder and the granulated one. Micrographs were taken at 2.7 KV and a working distance of approximately 12 mm. The images were taken at magnifications of 200X, 500X, 1KX, and 1.5KX.

2.2. Preparation of alumina slurries.

A total of 91 samples were prepared, and our results depend on some of them. Therefore, in the method section sample numbers are shown in unarranged series of numbers.

2.2.1. Ball milling

Ball milling was performed to reduce the particle size of the received powders. The BM-0801 mill with rollers and a motor was used at 180, 250, and 350 RPM. The duration of milling was 30 minutes, 1 hour, 6 hours, and 12 hours. Pure alumina milling balls with a diameter of 20 mm (99.7% purity, Friatec, Germany) were used in a container with a diameter of 155 mm.

2.2.2. Mixing ingredients (First stage)

Binders, lubricants, and alumina powders were added one by one to warm distilled water at 60℃. The mixture was stirred using a magnetic stirrer (ARE VELP Scientifica) and heated. The entire mixture was stirred for at least 30 minutes. Table 4 shows the amounts and concentrations of the materials used. Six groups of similar samples were prepared, with one parameter changing in each group while the other variables were kept constant. The main variable being changed was always increasing from the first sample to the last one in the same group. The variables included solid load, binder type and amount, and lubricant type and amount. Despite having similar properties in all slurry samples, different spray drying conditions were used.

Another sample group other than the shown in the table is prepared with $NaNO_3$ in 3000, 4000, and 5000 ppm added to the slurry. (Table 3)

Table 3. spray dried samples with $NaNO_3$ as a deflocculant.

	composition of the mixture				spray drayer parameters						
	solvent	**solvent**	**binder**	**lubricant**	**inlet temperature**	**outlet temperature**	**fan speed**	**compressed air pressure**	**spin cleaning**	**wriggle pump (feed)**	**Nozzle size**
59	DIS-water	40% m	1.5% PVA	0.5% PEG 400	270	87.5-90	100	0.11	1	40	1.5
60	DIS-water	40% M	1.5% PVA	0.5% PEG 400	270	90	100	0.11	1	40	1.5
61	DIS-water	40% M	1.5% PVA	0.5% PEG 400	270	92-100	100	0.11	1	40	1.5
62	DIS-water	40% M	1.5% PVA	0.5% PEG 400	270	82	100	0.11	1	40	1.5

Table 4. Ingredients of slurry parameters for each sample and in groups

Sample		Composition of the slurry				
		Solute of α-Al_2O_3	Binder		Lubricant	
Group	no.	(wt%)	(%)	Type	(%)	Type
Random Group (RG)	40 41 42 43	40	3.00	PVA	1.00	PEG 400
Group 1 (G1)	50	10	1.50	PVA	0.50	PEG 400
	51	20				
	52	30				
	53	40				
	54	50				
	55	60	failed because the nozzle clogged			
Mixed flow Group(MF)	63 69	45	1.50	PVA	0.50	PEG 400
Group 2 (G2)	73	35	1.50	PVA	0.50	PEG 6000
	74		3.00		1.00	
	75		7.50		2.50	
	76		9.00		3.00	
	77		12.00		4.00	
	78A		15.00		5.00	
	78B		15.00		5.00	
Group 3 (G3)	79 80 81 82 83 84	35	1.50	PVA	0.50	PEG 400
Group 4 (G4)	85 86 87 88 89 90 91	40	1.50	PVA	0.50	PEG 400

2.3. Spray drying (first stage)

Spray dryer TFS-2L (Tefic BIOTECH CO, China) was used in different variety of parameters. For each group of prepared samples, parameters were even the same or gradually changing. Table 5 describes the all conditions of spray drying.

In G3 temperature changed from 220℃ to 280℃, increasing by 10℃ from 79 to 84. In G4 atomizing pressure was increased by 0.2 MPastarting from 0.08 MPa at 85. Sample till 0.20 Mpa at 91. sample.

Table 5. Spray dryer parameters' values for each sample and in groups

Sample		Spray dryer parameters					
		Inlet temperature	Outlet Temperature	Fan speed (% of 2800 RPM)	Atomizing pressure	Rate of feed	Nozzle diameter
Group	no.	℃	℃		Mpa	mL/min	mm
Random Group (RG)	40	230	100-110	90	0.10	12	0.75
	41	240		90			
	42	220		100			
	43	220		90			
Group 1 (G1)	50	270	97-109	100	0.10	16	1.5
	51						
	52						
	53						
	54						
	55	failed because the nozzle clogged					
Mixed flow Group(MF)	63	280	100.00	100	0.20	12	1.5
	69		100-110		0.08	16	
Group 2 (G2)	73	220	95-100	100	0.12	8	0.75
	74						
	75						
	76						
	77						
	78A						
	78B				0.14		
Group 3 (G3)	79	220	85.00	100	0.12	12	0.75
	80	230	85.00				
	81	240	90.00				
	82	250	100.00				
	83	260	102.00				
	84	270	106.00				
Group 4 (G4)	85	270	95-100	100	0.08	12	0.75
	86				0.10		
	87				0.12		
	88				0.14		
	89				0.16		
	90				0.18		
	91				0.20		

2.4. Mixing ingredient and spray drying (Second stage)

After the first investigation, Deeper investigation was planned to prepare more samples and do tests to have better outcome of this research. In this stage slurry parameters were the main focus and how to adjust them in scientific plan.

The following table 6 shows how we checked the change of the solid load in the slurry, and the change of the binder type/amount, finally the change of the ratio of lubricant to binder amount.

2.1. Characterization

2.1.1. Flowability

Flowability was measured using the angle of repose method. A commercial cone with a 1 cm diameter opening at the end was placed vertically 4 cm above a flat surface of paper. The granules were allowed to fall freely from the cone to the flat surface, and the angle of repose was measured (Table 7).

Table 6. The angle of repose and the flowability description

The angle of Repose (°)	flow property
25-30	Excellent
31-35	Good
36-40	Fair
41-45	passable
46-55	poor
56-65	very poor
>66	very very poor

Table 7. Second stage of mixing ingredients.

Sample		Slurry Parameters					Machine Parameters				
		Solid load Al_2O_3	Binder		Lubricant		Inlet temperature	Fan speed (% of 2800 RPM)	Atomizing pressure	Rate of feed	Nozzle diameter
Group	no.	(wt%)	(%)	Type	(%)	Type	℃		Mpa	mL/min	mm
Solid load	10% 20% 30% 40% 45% 50% 55%	10 20 30 40 45 50 55	1.50	PVA	0.50	PEG 400	270	100	0.11	16	1.5
Type of Lubricant	PEG 400 PEG 1500 PEG 4000 PEG 6000	50	1.50	PVA	0.50	PEG 400 PEG1500 PEG4000 PEG6000	270	100	0.11	16	1.5
Ratio of PEG/PVA	0/2 0.5/1.5 1/1 1.5/0.5 2/0	50	2 1.5 1 0.5 0	PVA	0 0.5 1 1.5 2	PEG 400	270	100	0.11	16	1.5
Amount of total Binder and lubricant	2% 4% 6% 8% 10%	50	1.50 3 4.5 6 7.5	PVA	0.50 1 1.5 2 2.5	PEG 400	270	100	0.11	16	1.5

2.1.2. Particle size analysis

Particle size analysis was done on the granulated particles by dispersing a measured amount of 50 mg in distilled water. Mastersizer 3000 (Mastersizer 3000, Malvern, United Kingdom) laser diffraction particle size analyzer was used to measure the particle size distribution of granulated powders.

2.1.3. Microstructure analysis of the granules.

The morphologies and shapes of the granules were imaged by SEM (Leo Supra 35 VP FEG SEM, Zeiss, Oberkochen, Germany). To observe the difference between morphologies of received powder and granulated one. Micrographs are taken in 2.7KV - 5KV and around 12mm working distance. Images were taken at magnifications of (200X, 500X, 1KX, and 1.5KX).

2.1.4. Crushability

Dry pressing was carried out using a hydraulic press (ONDER LIFT, Istanbul, Turkey). Granules with an approximate volume of 1.6 cm3 and apparent density were placed in the mold, which had a 20 mm height and a rounded base with a 5 mm radius.The pressing was performed up to 280 MPa. The height difference after pressing was measured to calculate a crushability index that can be used to compare between samples (table 8).

$$\text{Compressibility} = \left(\frac{D_{Final} - D_{Initial}}{D_{Final}}\right) * 100$$

Table 8. Compressibility % and the crushability description

compressibility (%)	crushability properties
>67	Excellent
56 to 66	Good
45 to 55	Fair
36 to 44	slightly poor
29 to 35	poor
26 to 28	very poor
<2.5	Extremely poor

2.2. Preparing and measuring green body density

The same crushability samples pressed and used as a green body ready for sintering. Then using the basic formula of density calculation, the measured weight of each sample was divided by its volume.

2.3. Sintering

The sintering process was conducted under air pressure in a tube furnace (PROTHERM Furnaces, Ankara, Turkey). The temperature was raised to 1600℃ at a rate of 2℃/min and the samples were held at 600℃ for 2 hours, at 1200℃ for 2 hours, at 1550℃ for 2 hours, and at 1600℃ for 5 hours. The samples were then cooled down at a rate of 7℃/min. The tube used in the furnace was made of high-purity alumina.

2.3.1. Measuring density

The densities of the sintered samples were calculated using the Archimedes method with distilled water. This method is based on the upward force created by a fluid when a solid body partially or completely sinks in it. The upward force is equal to the volume of the liquid displaced by the solid body. Measurements done in three stages:

- Weight the sample in the air.
- Weight the sample completely covered with distilled water.
- Calculating the density by the following equation.

$$V_s \times \rho_s \times g = W_{air}$$
$$V_s \times \rho_s \times g - V_s \times \rho_{H_2O} \times g = W_{H_2O}$$
$$\downarrow$$
$$\rho_s = \frac{W_{air} \times \rho_{H_2O}}{W_{air} - W_{H_2O}}$$

3. Results

3.1. Ball milling

Ball milling was conducted in different periods to understand the optimum duration of milling, table of the results is shown in table 9. Figure 23 shows the particle size analysis of each sample, where 6 hours of ball milling had a particle size distribution at D50 = 4.49 µm.

Table 9. Particle size analysis for different duration of ball milling.

Ball milling duration	Dx (50) (µm)
30 min BM	17.6
1 hr BM	5.54
6 hrs BM	4.94
12 hrs BM	3.23

Figure 23. PSA of ball milling for 30 minutes, 1 hour, 6 hours, and 12 hours.

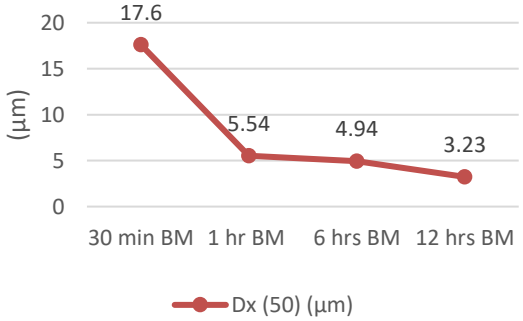

A variety of ball sizes and milling container bottles were used, to find the best conditions for milling as received powder. Between 6 different conditions of milling, 3 different sizes of Alumina/zirconia balls and 3 different container sizes were used (Table 10). The second condition's results had a good point to start spray drying. Figure 22 shows the D50 of the conducted particle size analysis on milled powders.

Table 10. Conducted ball milling in 6 conditions.

Sample	Ball diameter(mm)	Bottle diameter (mm)	RPM	D50 (µm)	Ball type
1	20	155	170	7.23	Alumina
2	20	155	340	4.95	Alumina
3	15	80	180	4.44	Alumina
4	15	90	220	4.07	Alumina
5	8	80	220	5.93	Alumina
6	15	90	180	4.44	Zirconia

Figure 24 particle size analysis of 6 different conditions of ball milling.

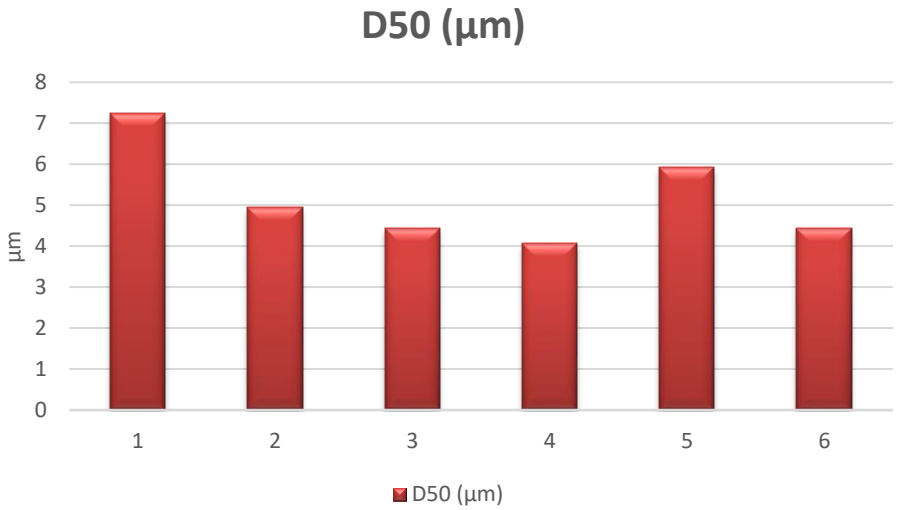

3.2. Spray drying (first stage)

Spray drying was done to granulate primary particles. Colors are used to show the data. Each group of samples was shown in one color, and for each group, there was one

variable increasing from one sample to another table 12. More details are written in the method section.

Table 11. labels of each group of samples.

Group	Label Color	Main changing variable	Samples no.
Random Group (RG)	Black	Random	40 – 43
Group 1 (G1)	Red	Solid load increasing	50 - 54
Mixed flow Group (MF)	Orange	Chamber design	63
Group 2 (G2)	Blue	PVA/PEG amount increasing	73 – 78B
Group 3 (G3)	Green	Temperature increasing	79 – 84
Group 4 (G4)	Purple	Atomizing pressure increasing	85 – 91

3.2.1. Collecting position

The collection of granules normally was done under the cyclone of the spray dryer in a collection bottle. There were many flying granules around the top of the drying chamber, observed during spray drying in the first tests. For each group of samples, a small, collected amount of those flying granules was conducted in our investigation. Promising-granules is the given name for those amounts. Granules collected from the collection bottle were not as nicely rounded as those collected from the upper part of the chamber. Figure 25 shows exactly where we could collect our samples.

3.2.1. Drying chambers

Mixed flow and co-current chamber designs were tested to understand the differences in the resulting granules. During our tests, the efficiency of the machine was affected by almost 30% down when a mixed-flow drying chamber was conducted.

Figure 25. Spray dryer Tefic TFS-2L, showing collecting promising sample position.

3.2.2. Nozzle size

More than explained before there are lots of samples. Among them, 2 samples had the same conditions except for nozzle size. Using different nozzle sizes of 1.5 / 0.75 mm in diameter showed a slight difference in the morphology of the particles. Table 13 shows the used ingredients for meant samples. Figure 26 shows the samples images in the microscope. The microstructure of the two samples in 500X is shown in figure 26. A/B.

Table 12. samples of different nozzle sizes.

Sample no.	Solid load	Binder	Lubricant	Inlet	outlet	Fan speed	Pressure of atomization	Feeding ml/min	Nozzle size
49	35%	3% PVA	1% PEG400	260	97	100	0.1	14	1.5
57				220	85	90	0.11		0.75

Figure 26. Samples' microstructure of granules made by a nozzle of diameter (A) 1.5 mm (B) 0.75 mm.

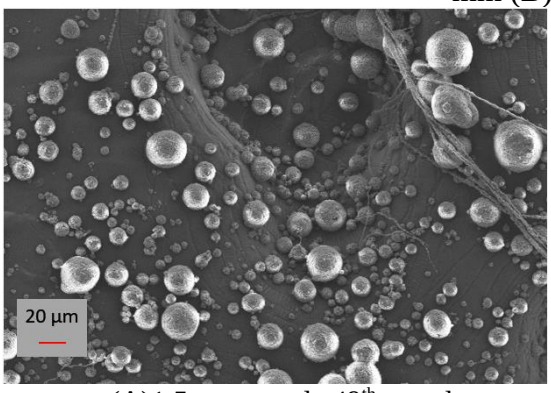

(A)1.5 mm nozzle 49th sample

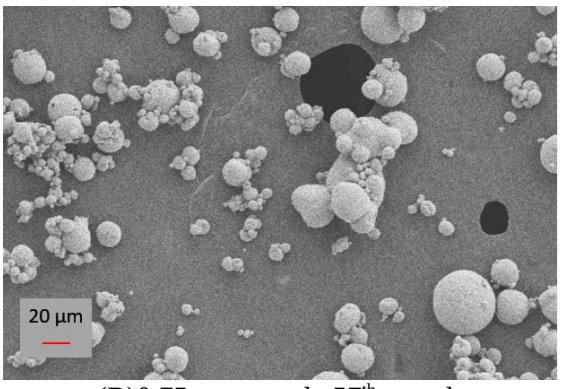

(B)0.75 mm nozzle 57th sample

3.2.3. Collected amounts.

The efficiency of the spray dryer was measured by measuring the collected amounts and calculating their percentages relative to the initially used powder amount. Figure 27 shows the efficiency of each sample in 3 different groups of samples. G2, G3, and G4 are shown respectively.

Figure 27. The efficiency of spray dryer for G2, G3, and G4 sample groups

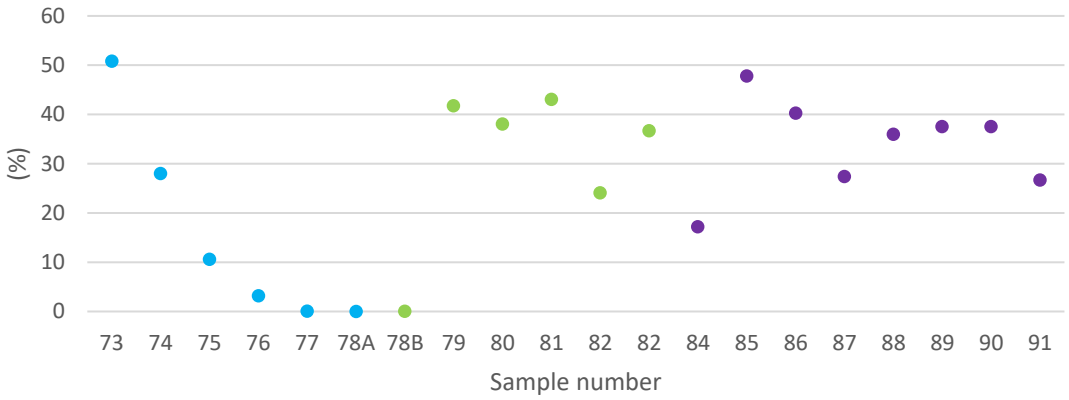

3.2.4. Outlet and energy consumption

3.2.5. Flowability

Flowability was measured by the repose angle method. The test was done and results are shown for the G1, MF, G2, G3, and G4 groups of samples in figure 28. promising-granules of MF, G3, and G4 are shown as the last column of each group.

3.2.1. Granule size analysis

Granule size analysis was done to figure out the particle size distribution and define the D50 of each sample. The test was done, and results are shown for the RG, G1,

MF, G2, G3, and G4 groups of samples. In figure 29 we can see the D50 value of each sample compared to the others. Measurement for promising-granule was also done for RG and MF groups.

Figure 28. flowability test, repose angle values for conducted samples.

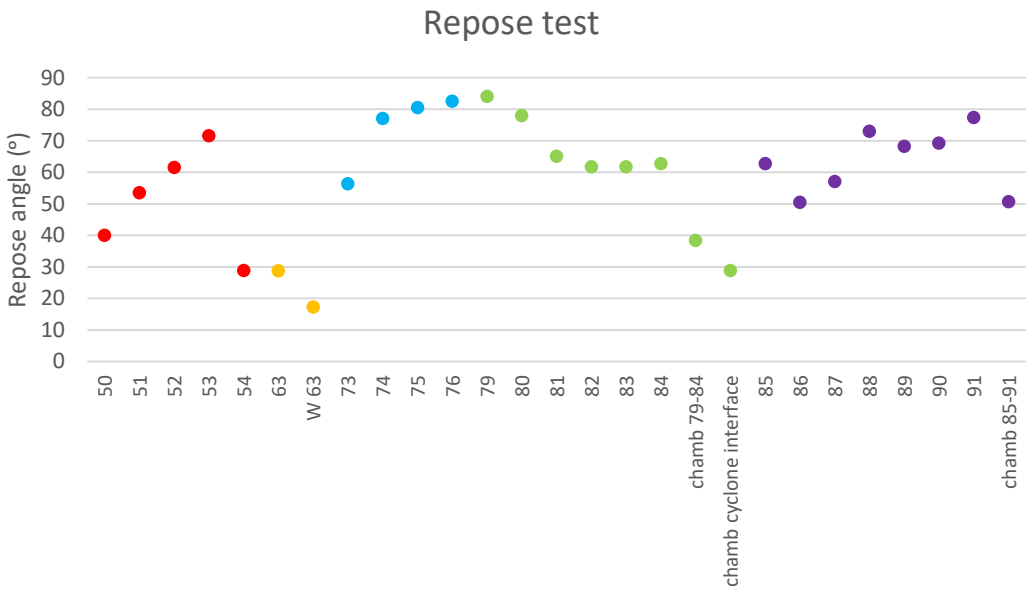

Figure 29. granule size analysis values for conducted samples.

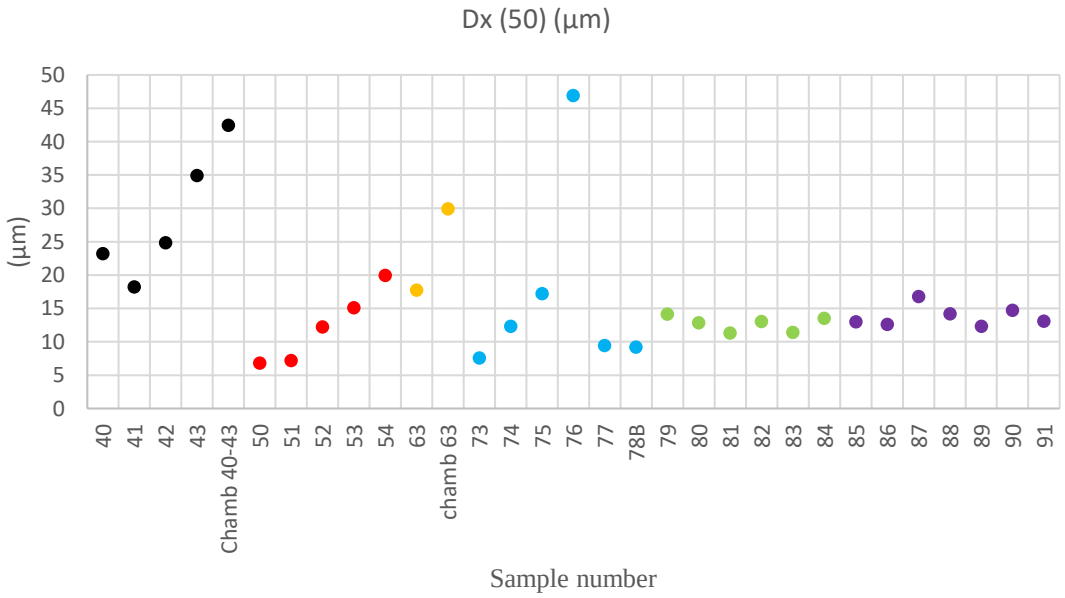

3.2.2. Microstructure

SEM was used to figure micrographs of the granules' shapes and surfaces. Samples of each group were imaged in different magnifications, to analyze their properties. In figure 30 granules that dried in a mixed flow chamber, the 63rd sample, and its promising-granule micrographs are shown in 1KX magnification. The same was done for the 69th sample, figure 31. Promising-granules for group 2 and group 3 are shown in figure 32.

In figure 33 microstructure and granule size are shown in 3 columns for 3 groups of samples. All micrographs are shown in 500X magnification. The variable parameter is written on the top of each column, while its value is defined on the right of each image. In figure 34, the microstructure of G2 is shown in 2 columns in a magnification of 1KX, and 200X. The variable parameter is written on the top of each column, while its value is defined on the right of each row.

Figure 30. Micrograph of mixed flow spray-dried granules

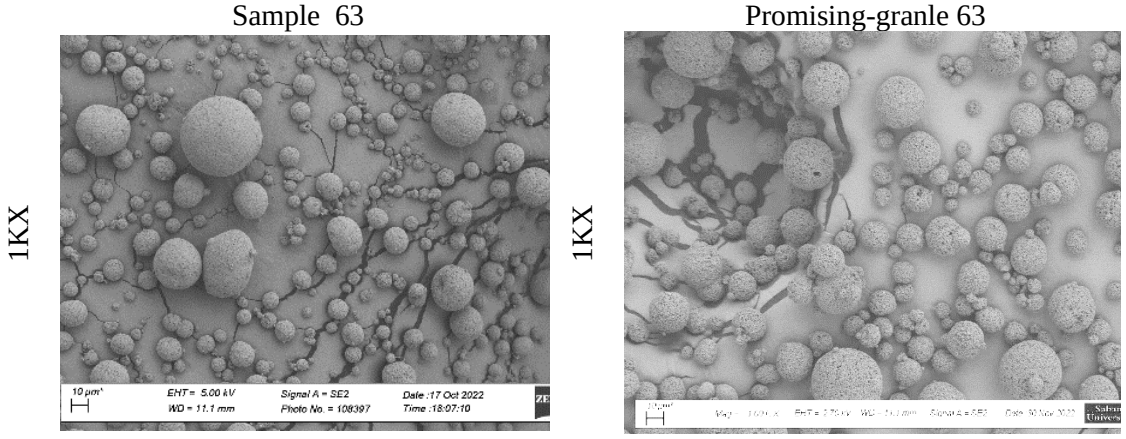

Figure 31. Micrograph of mixed flow dried granules

Sample 69

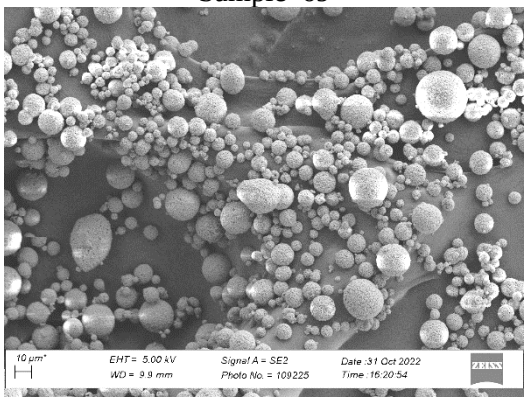

Promising-granle 69

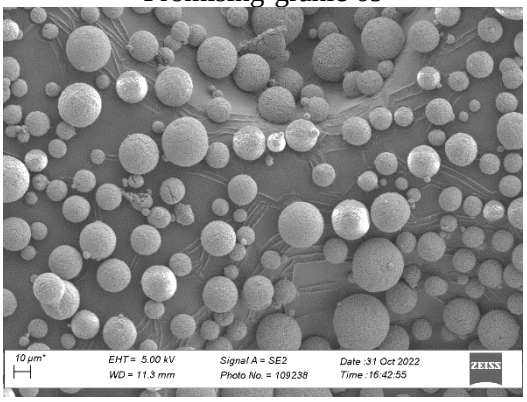

Figure 32. Micrographs of promising-granules for G2 and G3

Group G2 (promising-granule)

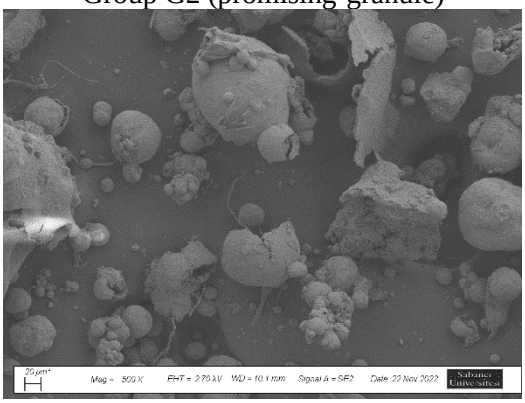

Group G3 (promising-granule)

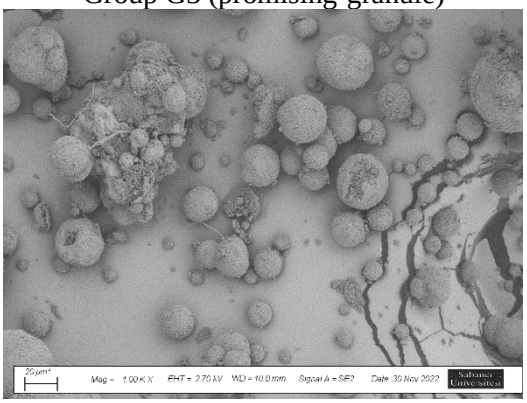

Figure 33. Micrographs of granules of G1, G3, and G4

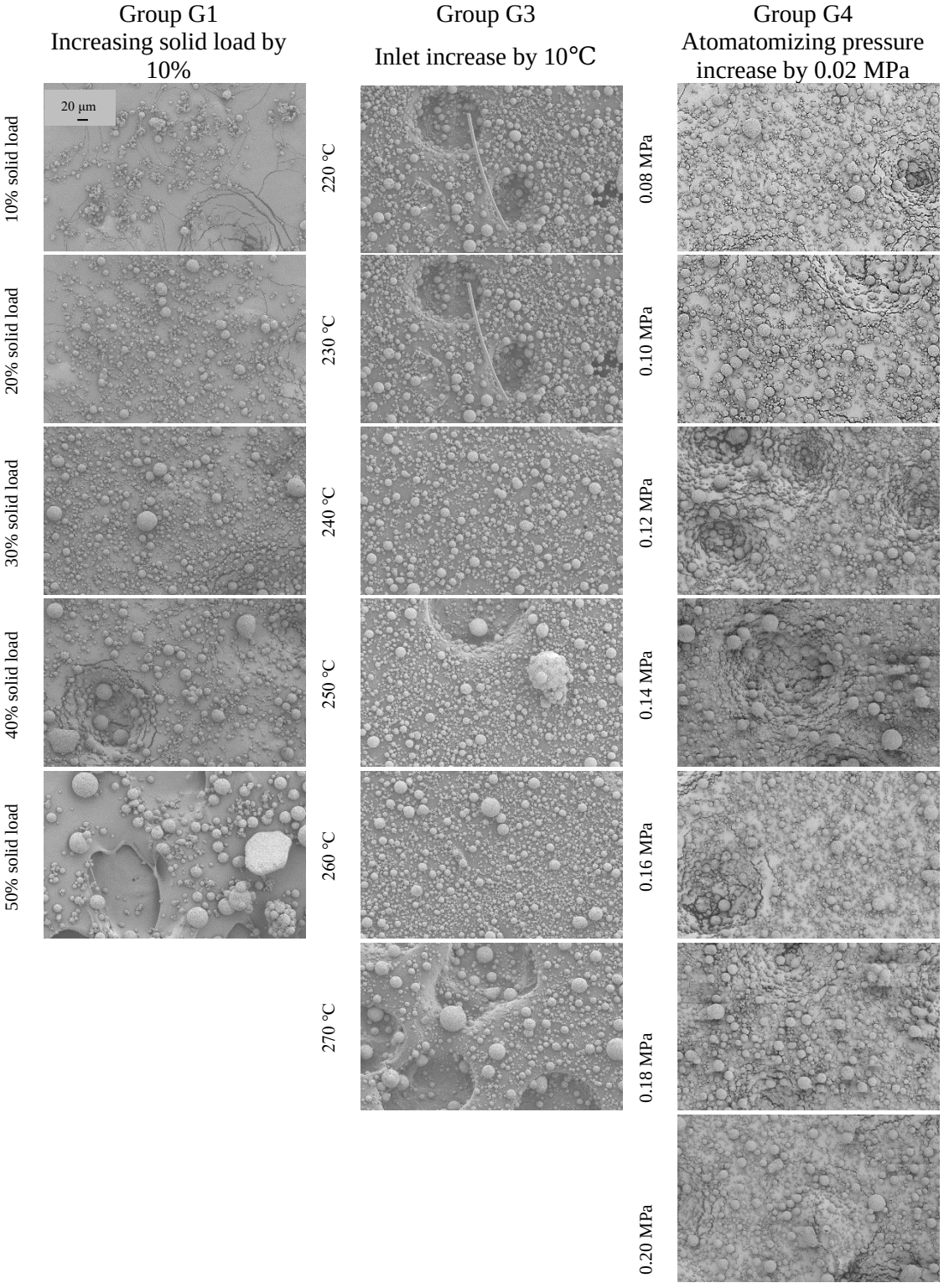

Figure 34. Micrographs of G2 in which an increment of PVA/PEG6000 was driven

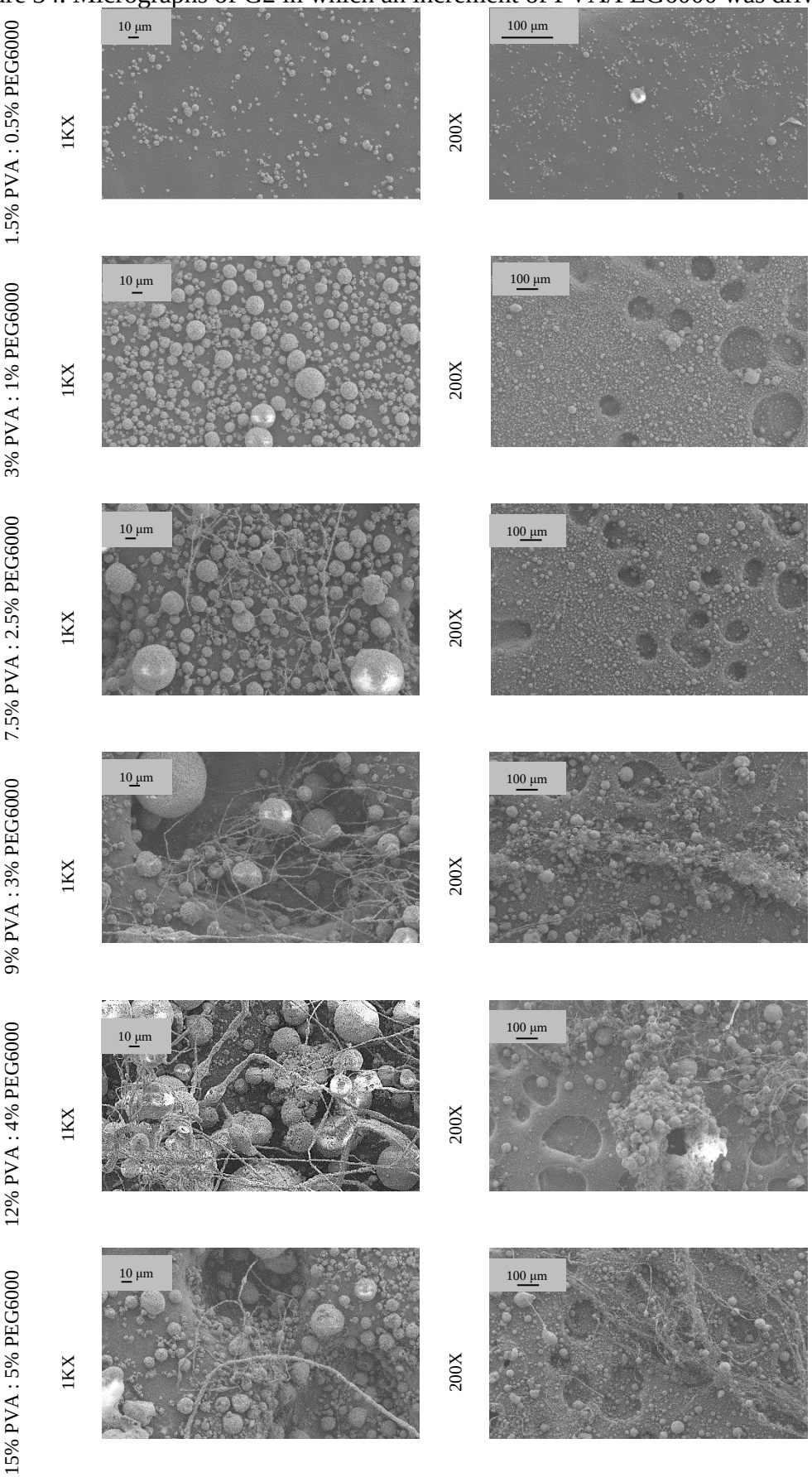

3.2.3. Crushability

A crushability test was conducted to determine the compatibility of granules. The results of the test are presented for the G1, MF, G2, G3, and G4 groups of samples. As shown in Figure 35, a number of samples had a crushability value of less than 30%, which is considered good based on the crushability formula. Promising granule samples from the G2, G3, and G4 groups were also included in this test.

Figure 35. Crushability test, values of crushability for 5 groups of samples.

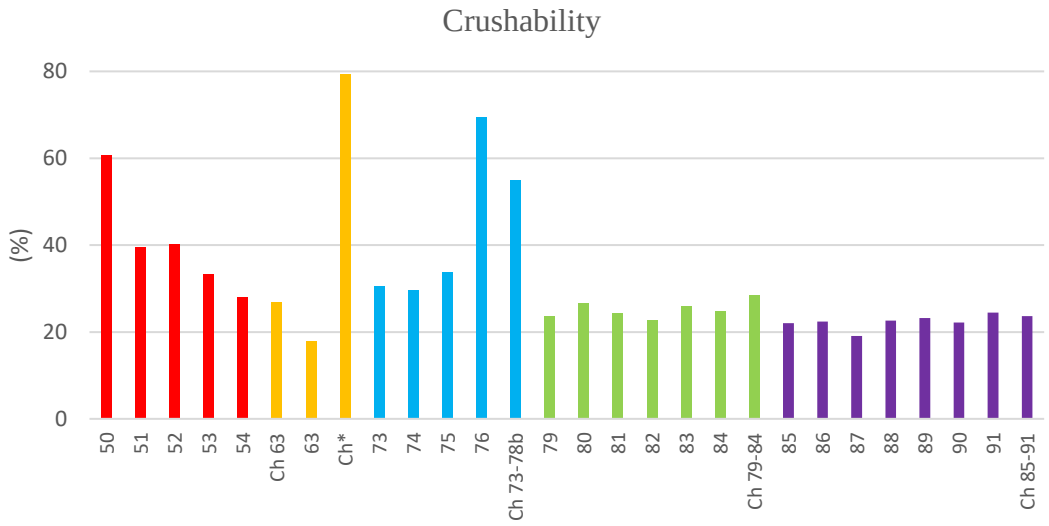

3.2.4. Green body density

The green density percentage was calculated from the theoretical density for all sample groups, including the promising granule sample of each group. The measurement results showed that the green density had a common value of more than 45% in most of the samples, and in three samples, it exceeded 50% of the theoretical value. Figure 36 displays the values of green body densities as a percentage.

Figure 36. Green density, The percentage of the green density of the theoretical density of alumina.

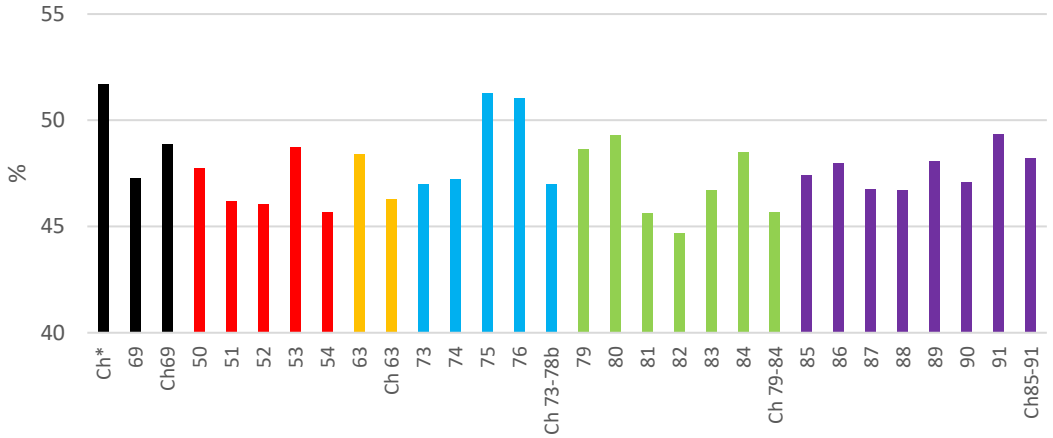

3.2.5. Sintered body density

sintered density percentage of the theoretical density. After sintering, density measurement was conducted again. Sintered density had a common value of over 96% in most of the samples and over 98% of the theoretical in 5 samples. Figure 37 shows the values of sintered body densities in percentage.

Figure 37. Green density, The percentage of the green density of the theoretical density of alumina.

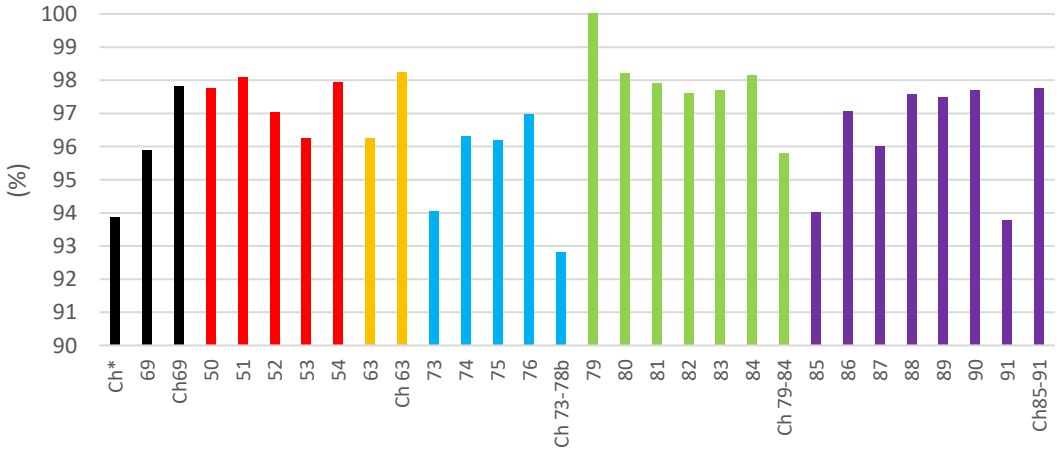

3.3. Spray drying (second stage)

In this stage an average of three conducted trails for each sample calculated. Therefore, final results collected all in the following table 13.

Table 13. results of the second stage tests.

sample name	green sample		Effeciency	Flowability	compressability	GSA		
	hight	mass		repos angle	calculated	D10	D50	D90
	mm	gram	%	degree	%		μm	
45m%	6.4	0.99	32.5	49.17	68	6	18	46
50m%	6.59	0.99	19.5	32.6	67.03	7	26	66
50% Solid load showed best properties								
PEG400	6.59	0.99	19.5	32.6	67.03	7	26	66
PEG1500	6.87	1.07	21.58	32.07	65.67	9	26	64
PEG4000	5.93	0.9	36.08	60	70.33	7	20	50
PEG6000	6.27	0.93	17.7	51.53	68.67	7	28	72
50% Solid load & PEG400 showed best properties								
0/2 % PEG/PVA	6.83	1.08	12.77	30.43	65.83	8	25	54
0.5/1.5 % PEG/PVA	6.59	0.99	19.5	32.6	67.03	7	26	66
1/1 % PEG/PVA	5.83	0.93	35	58	70.83	5	16	36
1.5/0.5 % PEG/PVA	4.97	0.79	28.5	65.33	75.17	4	12	30
2/0 % PEG/PVA	3.5	0.57	13.4	62.67	82.5	1	9	25

3.3.1. Granule size analysis

The granules produced from a 50% solid load had the largest size among all solid loads, as depicted in Figure 38.

The size of granules was found to be positively correlated with the size of the lubricant used. Smaller lubricants, such as those with shorter PEG lengths, led to larger granules figure 39. Same for PEG 6000 where agglomerated small granules shown as one big granule. But the real is that a sample with PEG 6000 as lubricant showed the smallest granules at the SEM images.

Finally, the ratio of lubricant to binder amount showed that 0.5/1.5 and 0/2 PEG/PVA had bigger granules comparing to the others figure 40.

Figure 38. Granule size distribution for different solid loads in slurry

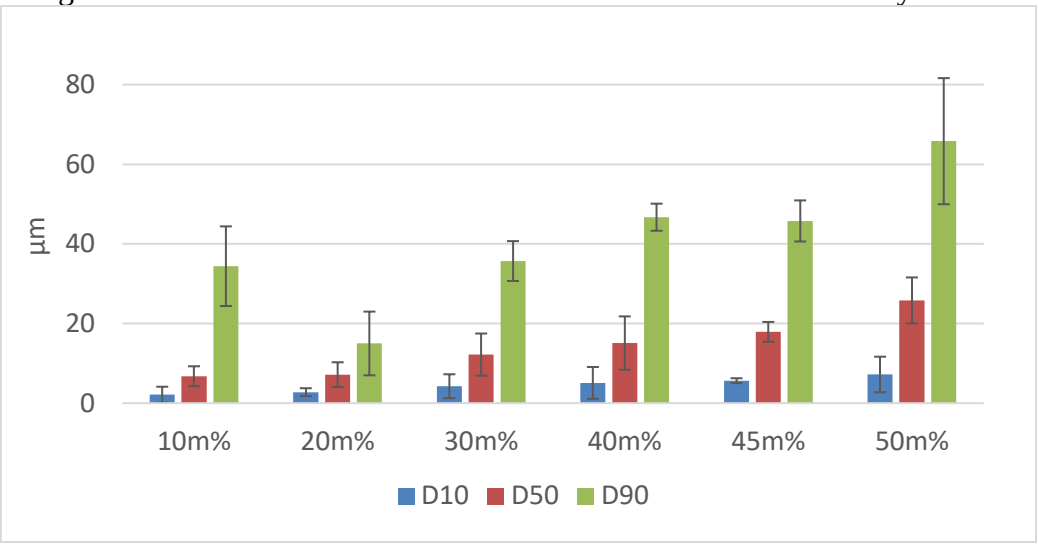

Figure 39. Granule size for 50% solid load but different lubricant type in the slurry

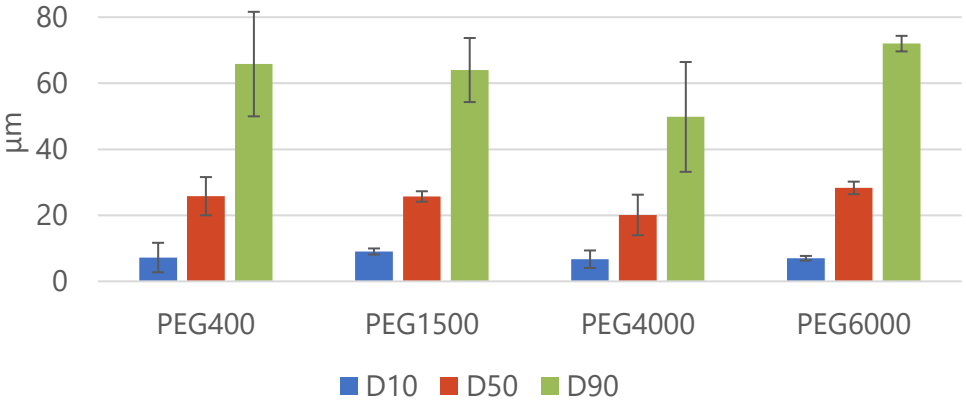

Figure 40. Granule size distribution for different ratios of lubricants to binders.

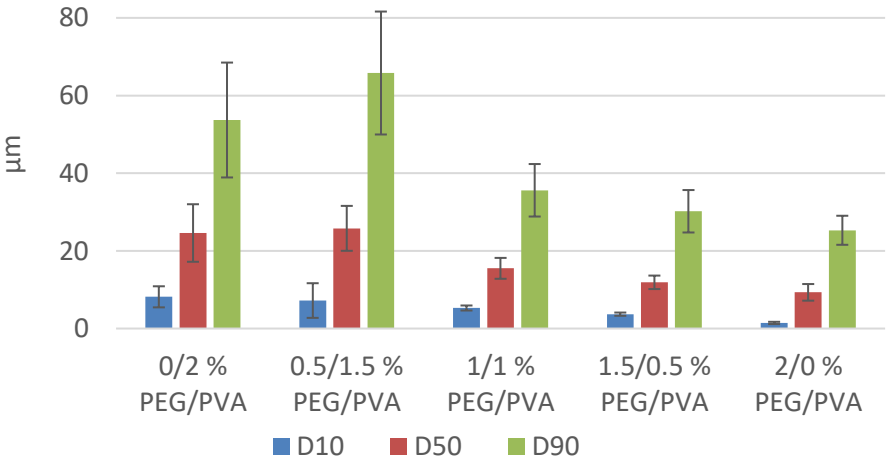

3.3.2. Flowability and crushability results

Figure 41. Crushability and flowability changing with changing in solid load

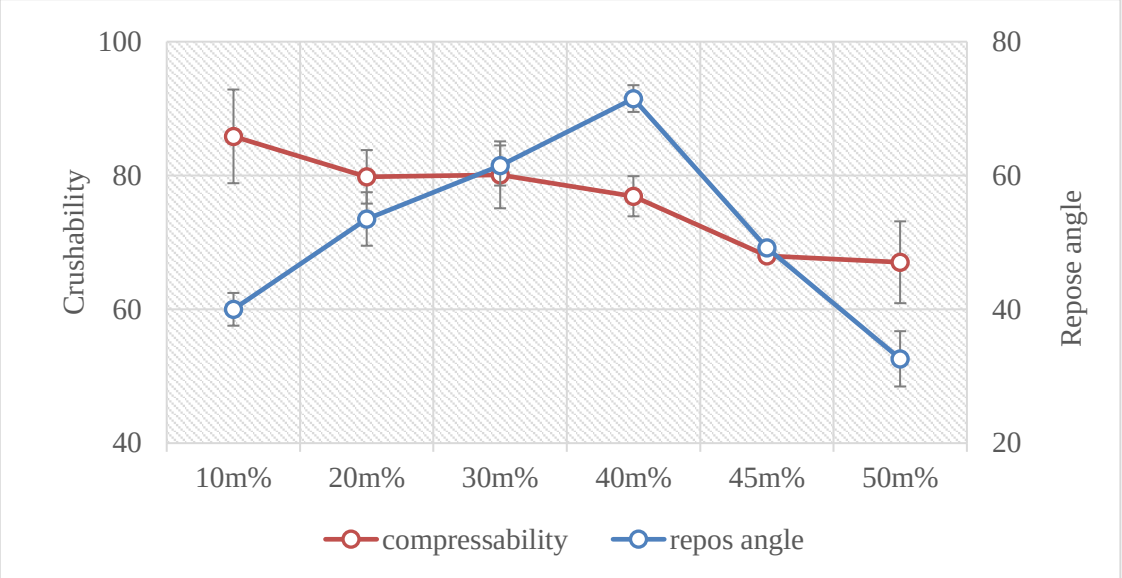

Figure 42. Crushability and flowability changing with changing in the lubricant type.

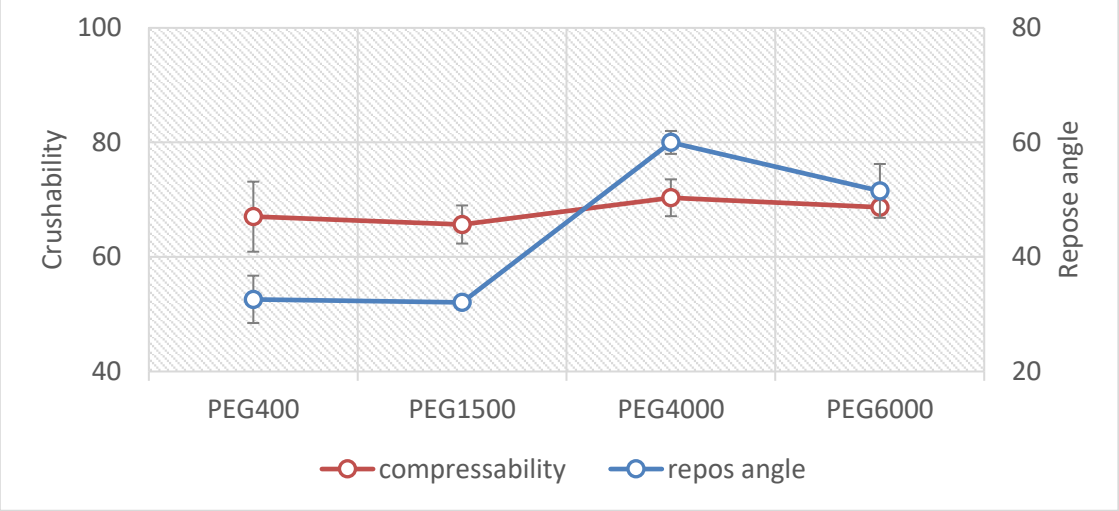

Figure 43. Crushability and flowability change with changing lubricant/binder ratio.

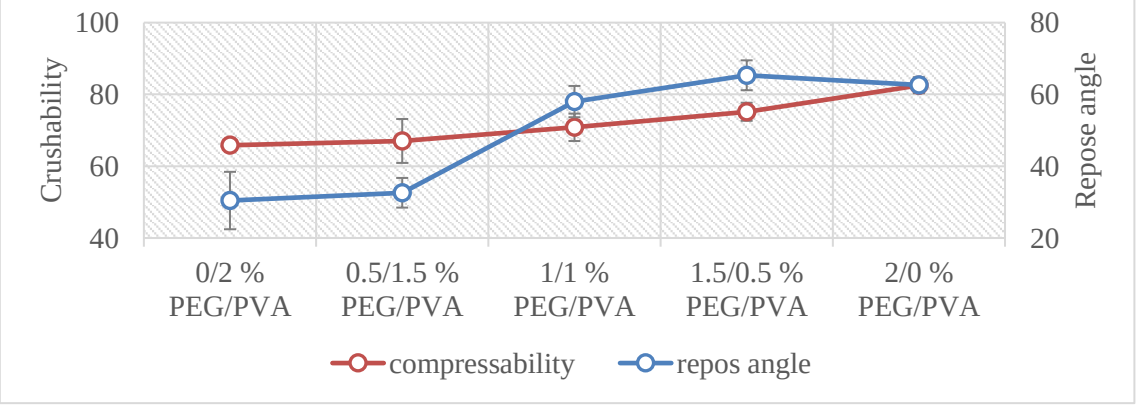

3.3.3. Microstructure

Increasing the solid load led to increase in the granule sizes. Figure 44 in 20 micron and figure 45 in 10 micron shows that.

Figure 44. Solid load change effect on the granules'' morphology. All images have 20 microns scale bar.

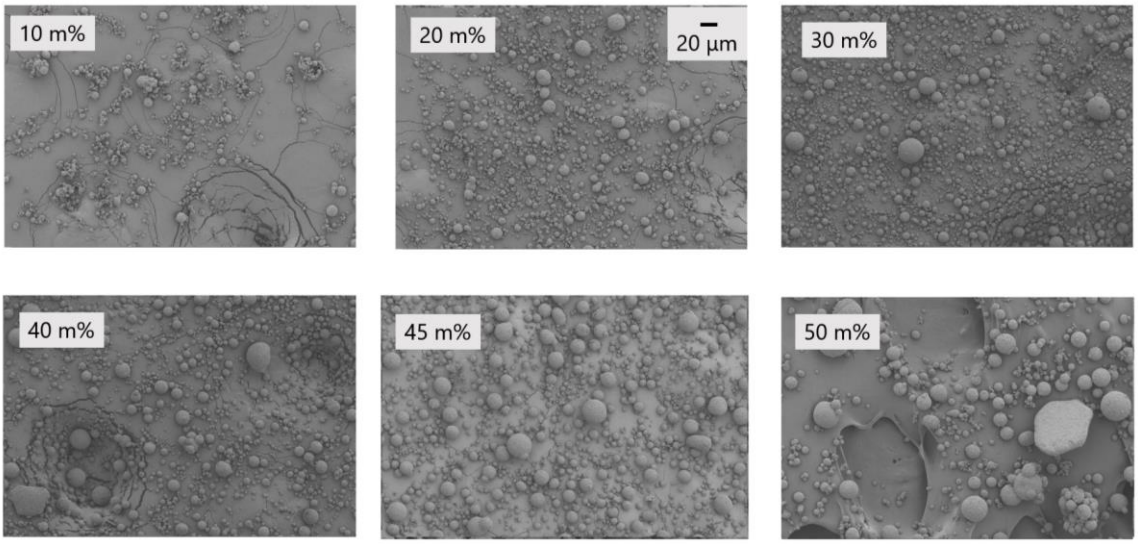

Figure 45Solid load change effect on the granules' morphology. All images have 10 microns scale bar.

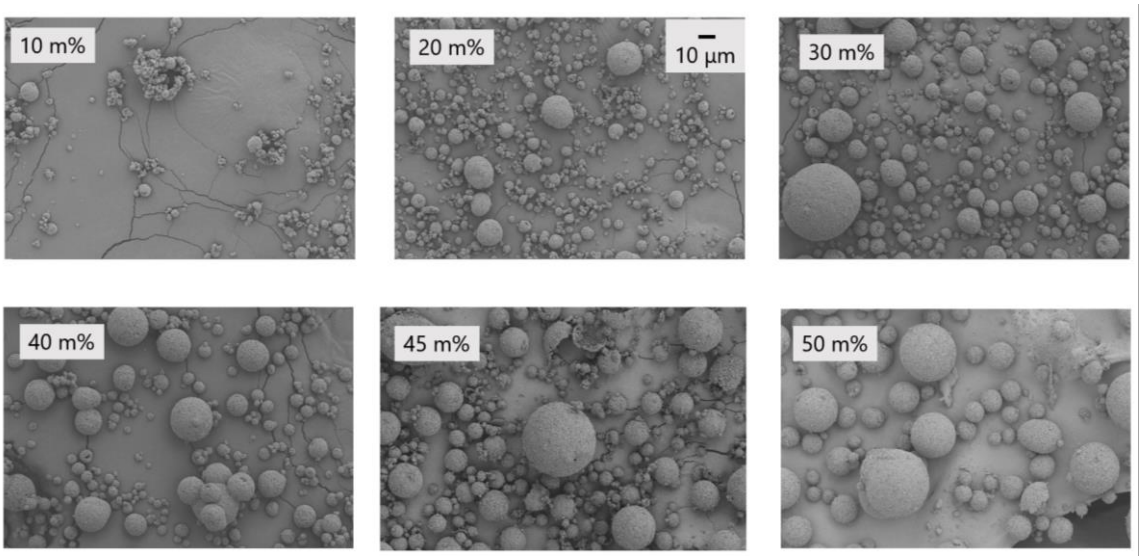

For the change in the type of lubricant. The short length lubricants of PEG 400 and PEG 1500 showed better and bigger granules. Comparing to the samples in which the lubricant length was 4000 PEG and 6000 PEG figure 46.

Figure 46. granules morphology changes with changing lubricant type. All images have 2 microns scale bar.

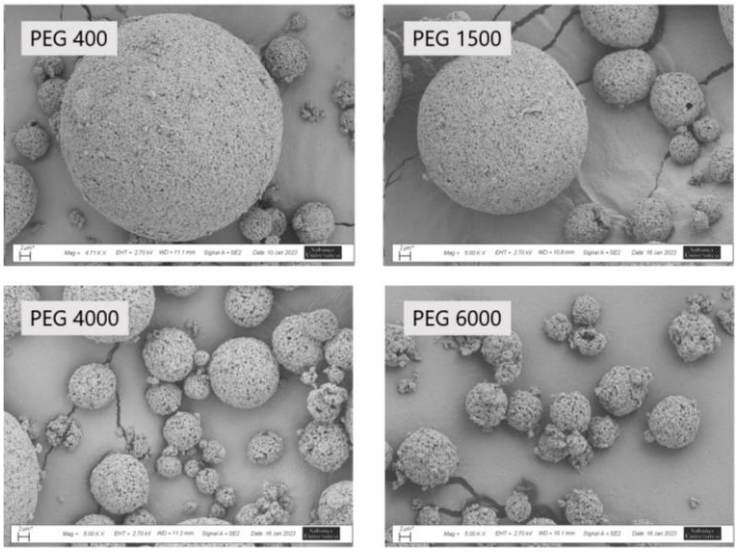

Changing in the ratio of lubricant percentage to the binder amount. Both as a percentage of the total Alumina amount figure 47.

Figure 47. Morphology changes with changing the lubricant/ binder ratio.

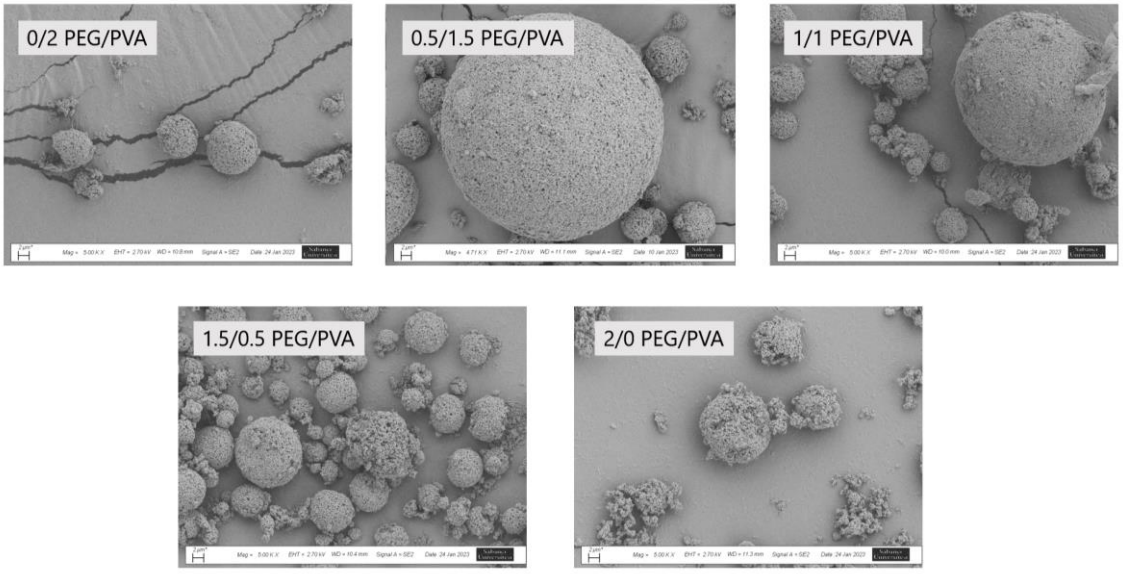

4. Discussion

4.1. Resulted relations (first stage).

4.1.1. Ball milling

Milling the powder before preparing granules was important, to reach an optimum particle size for the primary particles of granules. Powders were milled to different sizes and showed a further decrease in size with increasing the applied periods of milling. An applied period of 6 hours was chosen as a constant primary particle size for granulation.

Almost 5 μm size in D50 of the primary powder was reached while reaching 6 μm was advisable by Ramavath who tried 0.25 μm, 0.8 μm, and 6 μm of primary powders[31]. It is the opposite of the known rule of having fine particles for good sintering products[53]. sample number 2 in table 7 has a good point of starting after trying many sizes of Alumina balls and container bottles.

Used primary particle size did not affect the granulation process but it must influence the sintering and grain growth of the body.

4.1.2. Design of spray dryer

The design of the spray dryer was highly investigated for getting the highest efficiency of each type[6-8, 14, 52]. The efficiency of a spray dryer was mostly discussed from the perspective of the drying chamber and used nozzles.

While sticking to 3 designs of drying chambers was demanding in history, this study tried a new collecting position for mixed-flow and co-current flow chambers. The new position shown in figure 24 had given a nice granule (Promising-granules) with good properties to be explained in this section. Promising samples were shown better in figures 30, 31, and 38.

Figure 48. Promising granules of the 70th sample

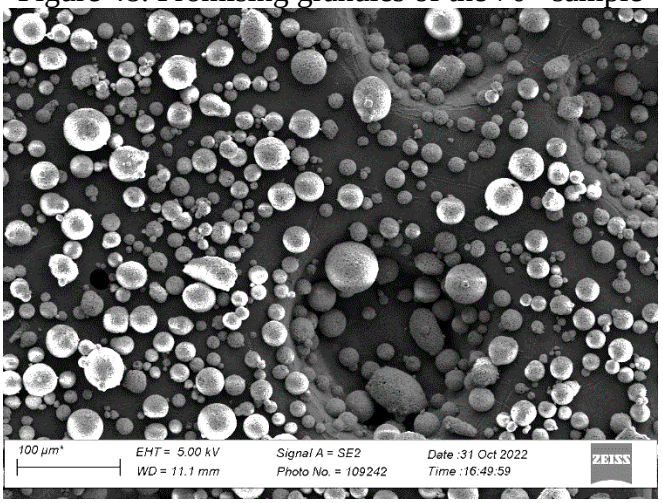

4.1.3. Granule size analysis

Particle size was increasing with the increase in the solid load at G1 samples. Figures 28 and 29 agree on that by looking at the microstructure and comparing it with the values of particle size of D50 for samples no 50 to 54. The size of particles, used a solid load of 50 wt.%, was almost 20 µm.

That agrees with the idea of increasing the amount of solid load will produce granules of bigger particles. As mentioned in [46] who used more than 70 wt.% solid load and got over 50 μm granules. Nevertheless, in [51] they used 51vol% solid load which in water correlates to almost 40 wt.% as the mentioned tap density is 39.9% of the theoretical density.

On the RG and MF group of samples, the promising particle size was bigger than the normally collected granules. Figures 31, 32, and 33 agree with these results. These results conduct with the rule of having the highest point of temperature in co-current at the top[14], promising-granules had a fair feeding rate value to dry instantly and fly from the nearest exit of the chamber because of the swirl drying air. The design of the co-current chamber mentioned having a swirl and laminar drying air ventilation [7].

In the G2 samples group, the given sizes correlate to the granules and ceramic fibers, those fibers were observed clearly in figure 34. The measurement of the 76th sample described the size of survived fibers in the PSA device well.

Temperature or pressure increase did not have a significant effect on the particle size but where the range of values was always between 10 μm to 16 μm. But comparing G3 with RG we had relatively lower temperatures but higher amounts of binders and lubricant that increased the particle size by decreasing the temperature. From that, we can agree on lowering the inlet temperature of spray drying results in better granules. Choosing the temperature of the inlet was discussed in [7, 14, 52] to balance between

higher evaporation degrees and lower temperatures to prevent thermal degradation of binders and lubricants.

4.1.4. Flowability

The mean flowability has decreased in G1, G2, and G4 by increasing the main variable of each group. While it increased in G3 with increasing temperature up to 240 ℃ where it started to stay constant for further heating. Promising-granules had shown always better flowability in MF, G3, and G4. In G2, granulation success necessed a maximum existence of 4 wt.% of binders-lubricants relative to the solid load weight. This agrees with the used amounts in literature[5, 16, 47, 50].

In G1, the increasing solid load led to have small particles that prevent the behavior of flowability. This was observed from the micrographs of the first column in figure 30. The meant micrographs are compared to the reasons for failing ball granules when having more than one size of granules and they are electrostatically attracted to each other. There are four types of structures that can be noticed in our micrographs (Coalescence, Breakage, Layering, and Abrasion transfer)[1] (figure 39).

G4 unflowability could be explained for the same reason shown in figure 39 and compared to the original samples of figure 30. In G2 which includes high amounts of binders and lubricants would naturally decrease the flowability value. this was obvious in the micrographs of figure 34.

Figure 49. Microstructures prevent granules from flowability. 53rd sample on the right

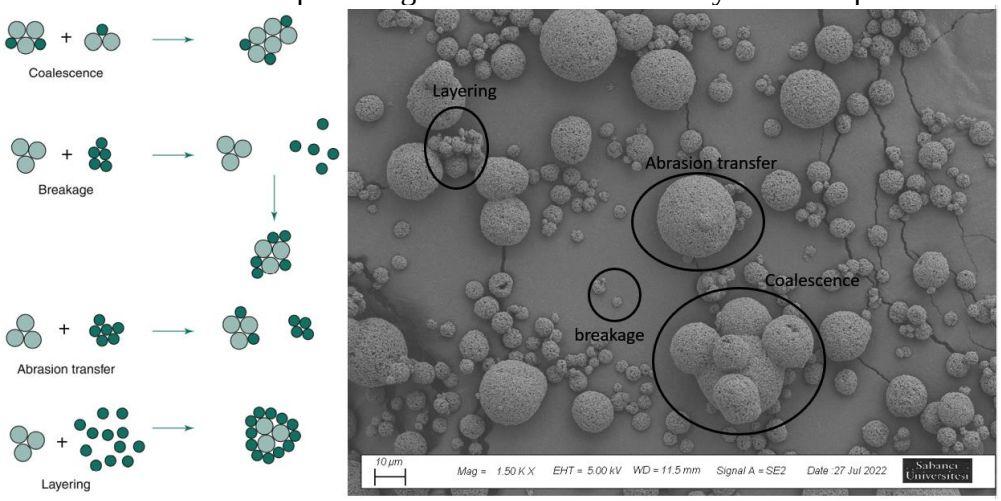

Increasing temperature added to the flowability of the granules because higher temperatures allow the collection of fully dried granules, and this was shown in the flowability of the granules[7]. The graph of flowability (figure 28) showed almost constant flowability along with increasing temperature after one value of 250 ℃. This means that the balanced temperature of the alumina granulation process is between 240 ℃ to 270 ℃for a co-current drying chamber. Table 2 shows that temperatures with values of 250℃, 260℃, and 300℃ were used in the literature. Promising-granules showed a nice flowability relative to the original samples. This can be understood regarding the PSA (figure 29) and better sphericity observed on microstructures like in figures 30-34.

4.1.5. Deflocculation effect

Adding NaNO3 was examined in 3000, 4000, and 5000 ppm in the slurry as a deflocculant, which decreased the PH of the slurry. Adding NaNO3 departed the connectivity between granules, which is observed in our all samples.

Figure 50. microstructure of samples with NaNO3 as deflocculant in the slurry

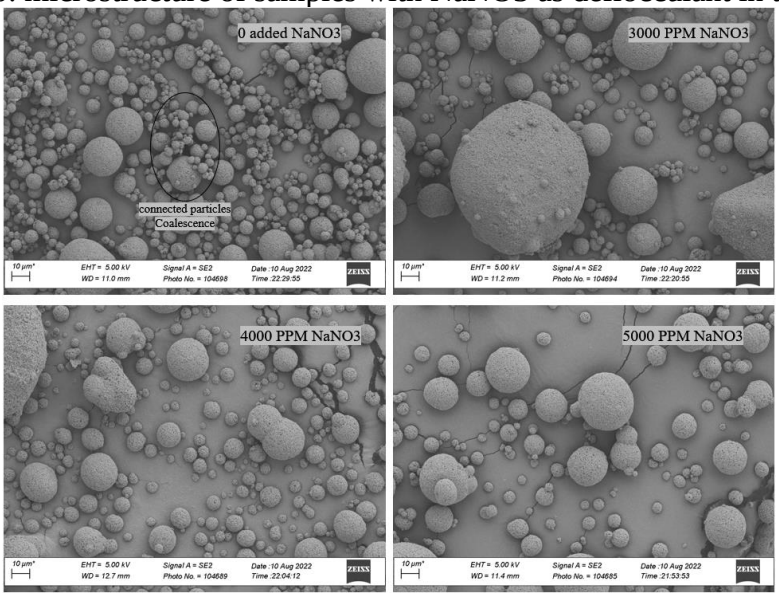

4.1.6. Binders and lubricants increasements.

In G2, increasing the percentage of PVA and PEG6000 added to the slurry. Fibers were so obvious in the chamber and cyclone separator during spray drying. The high amount of polymers exploded out of the droplet during drying and right after atomizing (figure 41), in a manner that the polymer breaks the droplet form, and at the same time the powder particles stick on the surface of the chamber. Nozzle size affected the amount of constructed fiber at a high PVA-PEG6000 with increasing the nozzle size.

Figure 51. Binder and lubricant increasement of the G2 samples.

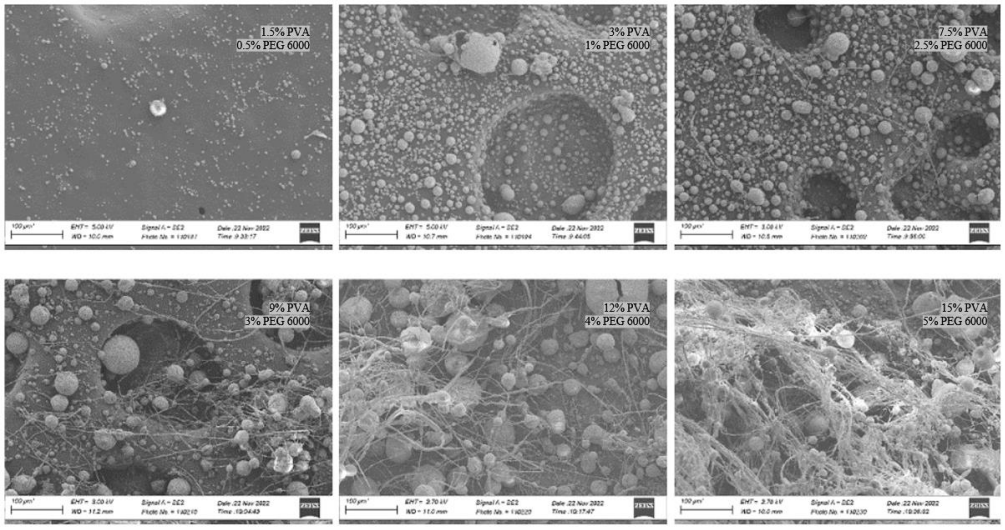

4.1.7. Crushability

Most of our samples had good crushability except those that included high amounts of binder and lubricant. Figure 35 shows crushability values were less than 30%. This can be explained by the inside voids created because of the capillary force. Capillary force affects the packing density inside granules, the possible packing density of granulation is between 6% to 65% percent, whereas in the ideal situation of spherical particles it comes up to 74%[30]. We could image the inside granules of some samples in figure 42.

Figure 52. Voids inside granules enhance crushability (a)Ch 73rd (b)6th (c)65th sample.

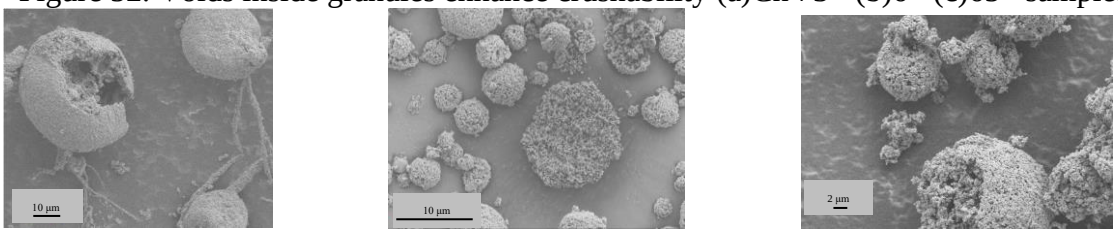

(a) (b) (c)

4.1.8. Green density and sinter density.

For G1 the mean green density of the samples is 47% of the theoretical densities. The relatively high green density of G2 was because of the weight of binders and lubricants inside the body, which burned out and affected the sintered body density. For the whole graph, increasing the green density at the samples has a reflection of the sintered density, in most of the samples. Exceptions could be explained by the amount of existing binder. Although the 63rd promising-granules has a green density less than the normal 63rd sample, its sintered density was better. This is depending on the good flowability, and bigger particle sizes owed by the 64th promising-granules.

Figure 53. Green density and sintered densities of the samples

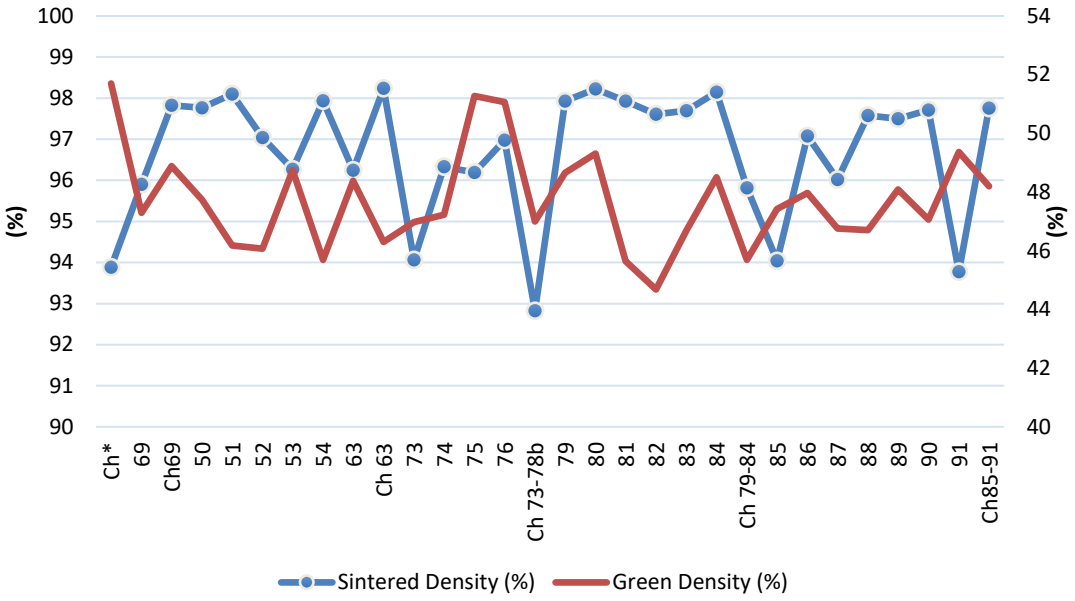

4.2. Correlated relations (first stage)

4.2.1. Crushability and flowability

The graph in Figure 44 demonstrates how the crushability value changes as the flowability value increases or decreases. Flowability influences the ease of filling the mold, while crushability measures the ease of crushing the material.

Figure 54. Flowability and crushability in the perspective of changing parameters

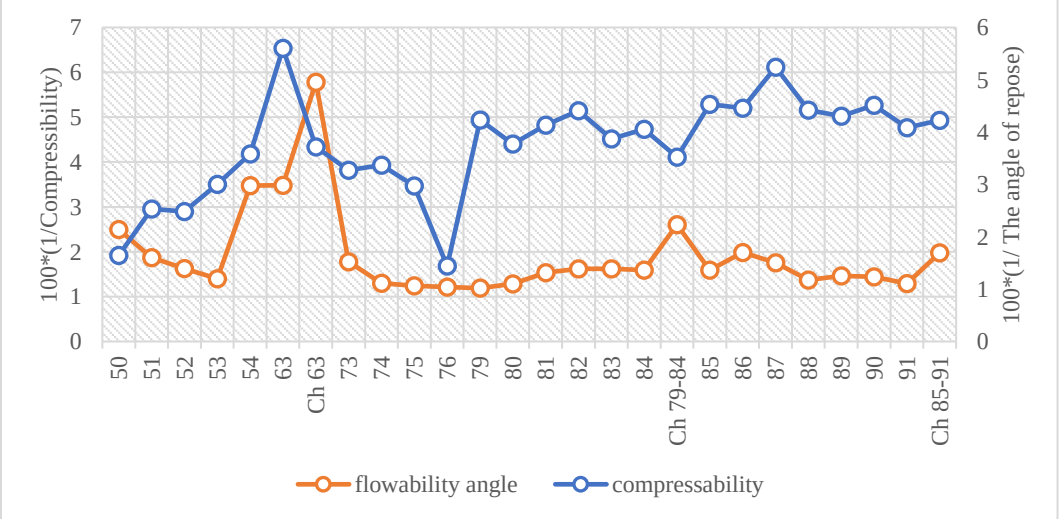

Despite the fact of two properties are increasing or decreasing together. In solid load increasing at G1 of samples we had increasing in compressibility although the flowability was decreasing. This is also could be explained by the same reason shown in figure 39.

4.2.2. Flowability and particle size analysis

The angle of repose value describes the value of flowability resistance. In G1 as the particle size increases with incresement in the solid load, flowability resistance increase. This can be explained that the device may have read coarser granules (Figure 45). The granules of the 63rd sample showed improved flowability as the granule size increased. This was due to the decrease in total surface area of the granules, which resulted in easier flowability.

Figure 55. Particle size analysis and flowability resistance relation in the perspective of changing parameters

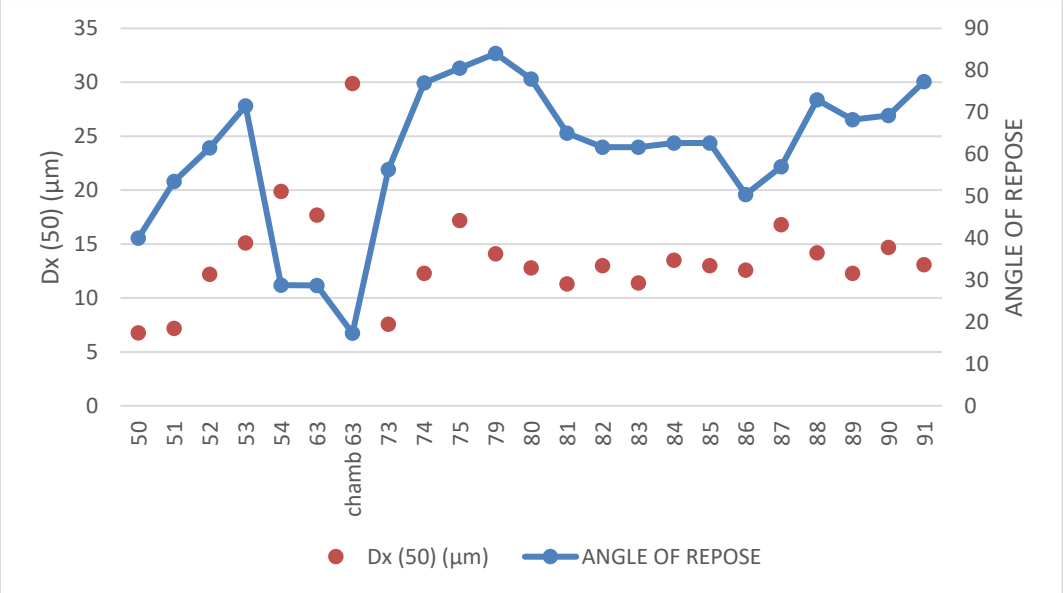

Increasing the amount of PVA and PEG6000 in G2 has a realistic effect on flowability resistance. As more binders are added, they inhibit the flowability of the particles. However, in G3, we observe a strange phenomenon: as the particle size decreases, flowability improves with an increase in temperature. This may be explained by the drying value of the resulting granules. Generally, a fully dried granule will flow better than a medium-dried one.

4.2.3. Crushability, Green density, and sintered density

Crushability is related to the sintered density directly and inversely to the green density.

Figure 56. Crushability effect on the green and sintered densities

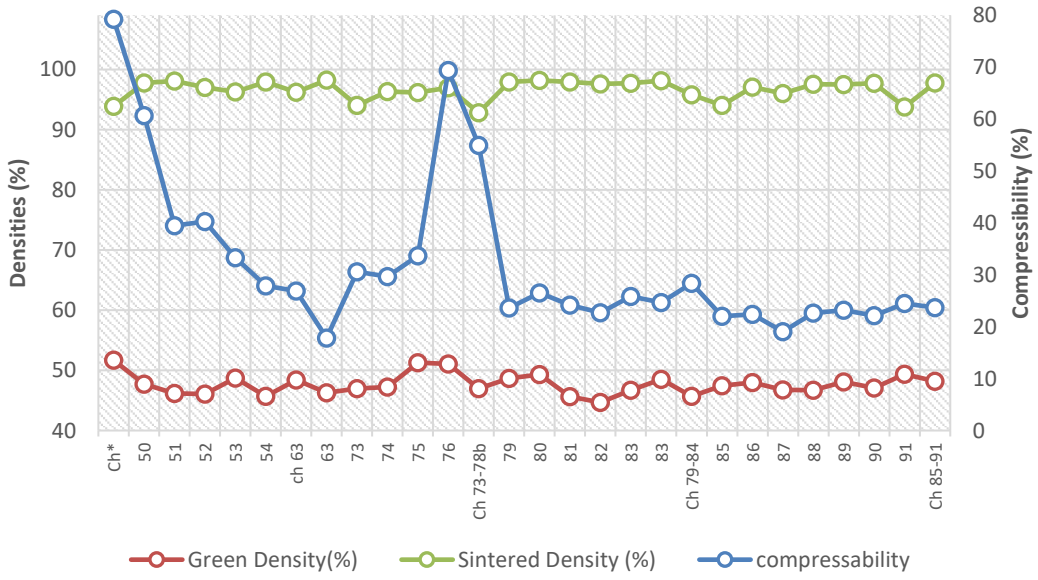

Existence of binders and lubricants more than 4% showed low compressibility value and that had a direct effect on the sintered density. This was clear at Ch* and ch 73-

78b as well. While the low described compressibility in 50 and 51 showed because incompletely spherical and small granules are there. That had its effect on the green density but not on the sintered density where un homogenous density could exist.

In the samples of G2 and G3, the flowability behavior shown in Figure 28 is inversely proportional to the sintered body density values shown in Figure 43. While it appears that decreasing density is correlated with increasing flowability, our samples were not sufficiently flowable to draw this conclusion. This could be an interesting topic for future research.

4.2.4. Collected amounts and efficiency of the spray dryer

The figure (48) shows the efficiency of the spray dryer during changing the machine parameters. A trend line explains how increasing the parameters decreases the efficiency of the machine. In the literature, it was mentioned that using the maximum available value of drying air flow rate increases the efficiency of the cyclone[7, 54].

Figure 57. Collecting efficiency of the machine with changing parameters

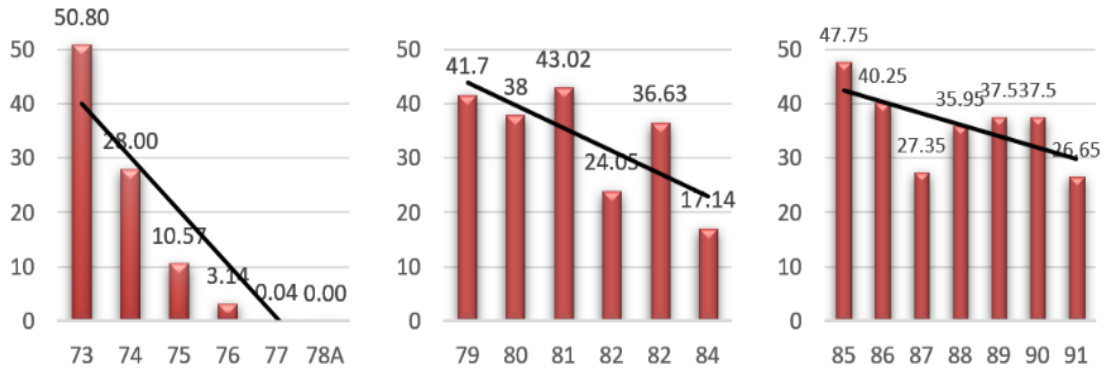

Collected amounts are more related to the machine parameters. as it is the indicator of the efficiency of the spray dryer.

4.2.5. Outlet temperature and efficiency of the spray dryer.

The outlet temperature of the spray dryer is derivatized by the inlet temperature, drying air flow rate, evaporation enthalpy of the solvent, and solid concentration in the liquid stream[7]. Figures 59 explains visually and by numbers this fact. The consumed energy during being in the chamber was high. And decreased by increasing temperature. Then showed almost a straight behavior on 61% of the inlet temperature.

Figure 58. Energy consumption efficiency of the machine with increasing inlet

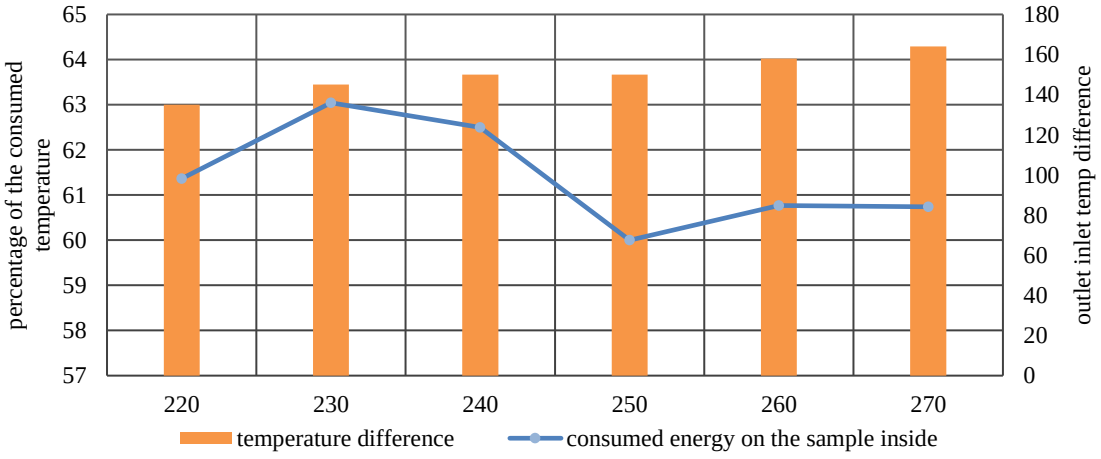

The consumed energy decreased because of the decreased amount of water to be evaporated by increasing the solid load in the samples.

4.3. Results of Second stage.

A change in the solid load leads to a corresponding change in the amount of water to be evaporated. As a result, a lower solid load within a droplet facilitates the likelihood of it being split by the fan and atomizing pressure within the chamber. It has been reported that an increase in the solid load has a highly positive effect on the size of the granules[7]. Stages of forming a droplet was shown in figure 6.

Figure 63 illustrates schematically the relationship between the observed images from the scanning electron microscope in Figures 44 and 45 and their impact on the flowability of the granules.

Figure 59. schematic of granules' morphology and how this led to having different granules' properties.

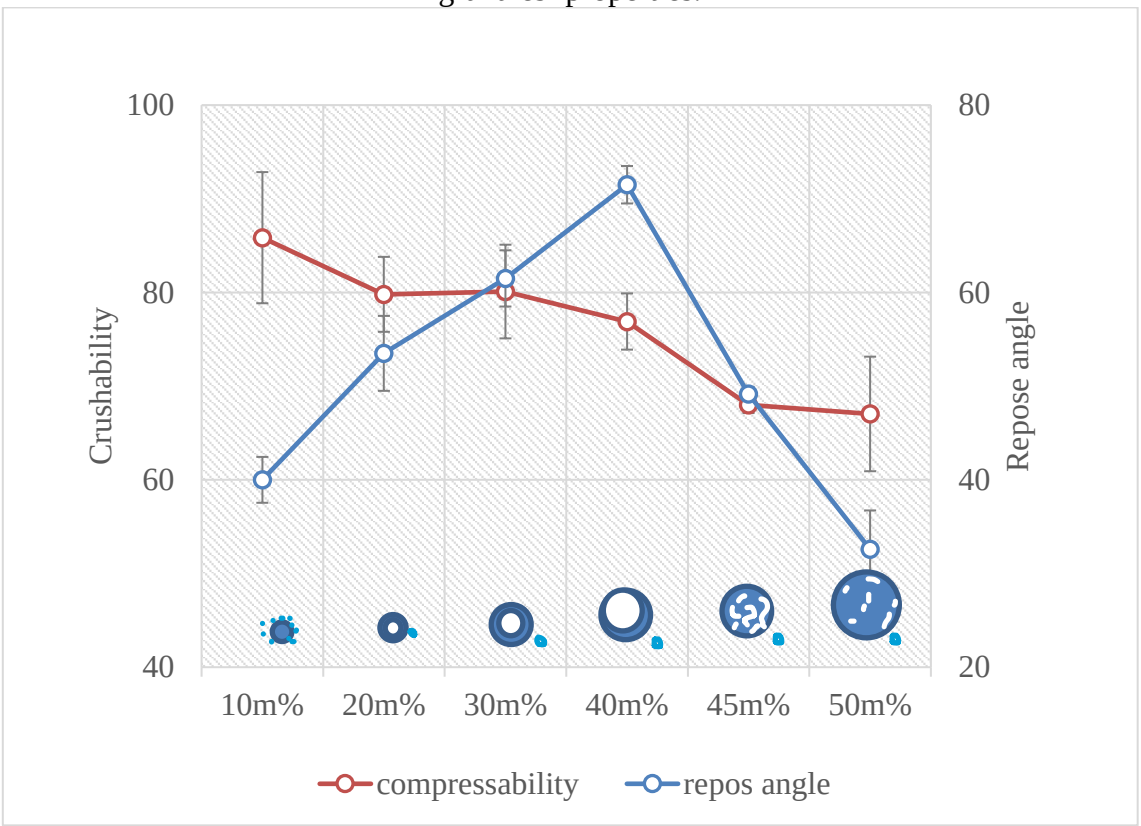

4.4. Polymers of the slurry in the second stage.

In this stage, the lubricant utilized is polyethylene glycol (PEG) and the binder is polyvinyl alcohol (PVA). Both have distinct chain structures as shown in Figure 64. The main difference lies in the presence of polar ends in PEG and a non-polar chain along its length, while PVA has a [OH]- along its polymer chain.

The attachment of polymers on the surface has been previously explained in Figure 18. As such, PEG attaches itself to the Alumina particle in a tail or loop form within the slurry, while PVA behaves like a train attachment in the slurry.

Figure 60. Chains of PEG and PVA

PEG PVA

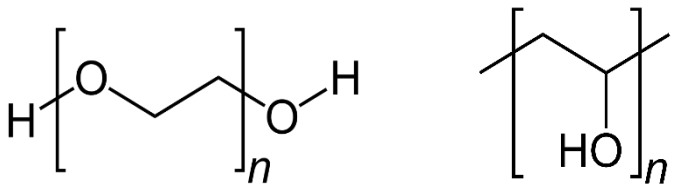

Looking to the resulted granules in figures 46 and 47. The explanation of having such granules is interpret the role of binder in granulation as a bridging polymer to bridge between powder particles and form granule spherical shape. While the role of having lubricant is to facilitate crushability and flowability. Figure 65 shows how PVA exist in one granule in red and how PEG behave between granules.

Figure 61. PEG between particles in green and PVA between particles in red

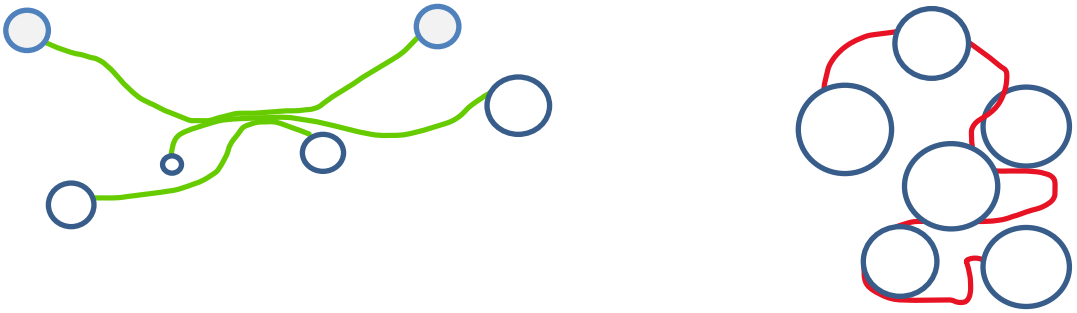

An increase in the length of PEG or its percentage as part of the total Alumina leads to the formation of ceramic fibers with interconnected morphologies and granules. Figure 66 shows PEG between granules in green and PVA between granules in red.

Figure 62. PEG between granules in green and PVA between granules in red

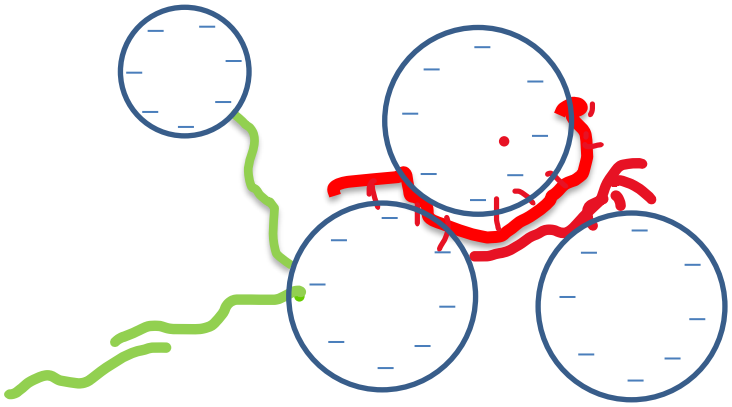

5. Conclusion

Granules has wide effect on ceramic processing and the properties of the final products. In this study the granulation of alumina powders was conducted in co-current and mixed flow spray dryer, to understand the granulation process of ceramic powders. During spray drying process many parameters and variables gradually changed, and their changing was reported.

A manual of understanding spray drying was illustrated in the results and discussion section. In this manual many points could kept in mind during making granules in ceramics.

- Ball milling: size of primary particles will not prevent granulation process, but will affect the sintering process later.
- Design of spray dryer: it was observed that the mixed flow design gave better granules in flowability, crushability, and sintering density. Draw back of the efficiency of collecting in the mixed-flow drying chamber design could be solved.
- Collecting bottle position of the granules in co-current drying chamber was not in the best position, or it is better to have two collecting positions, where different granules with different properties could be made.
- Promising-granules were collected from the top of the drying chamber. Which have best properties of flowability, crushability, and density of sintered bodies comparing to the normal samples.

- Inlet temperature of each slurry must be balanced depending on the used materials, especially binders and lubricants. Increasing inlet temperature has a positive influence on the flowability of the granules.

- High solid load of slurry increases the particle size and the density of the granule. Nevertheless, flowability decreased, this was clear because of the existence of coalescence, breakage, layering, and abrasion transfer in the microstructure of the granules.

- Deflocculation existence brought the existence of coalescence, breakage, layering, and abrasion transfer, in the microstructure of the granules to its minimum observed amount.

- Binders and lubricants presence weight percentage should not pass 4% of the used solid load in the slurry. Otherwise, ceramic fiber will exist around the granules.

- Crushability was observed to be high for most of the samples. Granules have voids inside their microstructure that adds to the crushability property. Binders and lubricants existence, after a maximum amount of 4% weight relative to solid load weight, in the granules structure showed decreasing in the crushability and resulted sintered density.

- High sintered density over 98% of alumina pellets of the theoretical density were made. 80^{th} and 84^{th} sample done at inlet temperature of 230℃ 270 ℃, 63^{rd} promising-granules collected from the drying chamber, and 51^{st} with 20% solid load slurry are the noticed high-density samples.

Finally, using 45% or 50% solid load with 0.5% short length PEG 400 as lubricant and 1.5% PVA for bridging in granulation gives the best properties of resulted granules.

After understanding the effect of changing granulation parameters on ceramics, perfect crushability, green density and sintered density to be brought to higher levels in a future studies. Keeping in mind the parameters effect handout which delivered in this study.

Future work

- Trying ethylene glycol as a lubricant
- Using Alcohol as a solvent and see how this would affect the granulation, as the evaporation point for alcohol is lower than water.
- Trying many creative designs would be a future work.
- Comparing different suspensions like citric acid, polyelectrolytes acid, and NaNO3 influence on the granulation of alumina or ceramics in generals is a new idea for future work.
- Preparing ceramic fibers by spray drying is a great idea for a future work.
- A study can be done on a composition of two or more ceramic materials granulation. Composites like MgO-ZrO_2 or Al_2O_3-ZrO_2 would be a key factor for such a study.

6. Reference

1. Aulton, M.E., *Powders, granules and granulation.* Aulton's Pharmaceutics E-Book: The Design and Manufacture of Medicines, 2017: p. 476.
2. Francis, L.F., *Powder processes*, in *Materials processing: a unified approach to processing of metals, ceramics and polymers*. 2016, Elsevier. p. 343-414.
3. Svarovsky, L., *Characterization of powders*. 1990: John Wiley & Sons: Chichester.
4. Eskandari, A., et al., *Effect of high energy ball milling on compressibility and sintering behavior of alumina nanoparticles.* Ceramics International, 2012. **38**(4): p. 2627-2632.
5. Bertrand, G., et al., *Spray-dried ceramic powders: A quantitative correlation between slurry characteristics and shapes of the granules.* Chemical Engineering Science, 2005. **60**(1): p. 95-102.
6. Anandharamakrishnan, C., *Spray drying techniques for food ingredient encapsulation*. 2015: John Wiley & Sons.
7. Cal, K. and K. Sollohub, *Spray drying technique. I: Hardware and process parameters.* Journal of pharmaceutical sciences, 2010. **99**(2): p. 575-586.
8. Lukasiewicz, S.J., *Spray-drying ceramic powders.* Journal of the American Ceramic Society, 1989. **72**(4): p. 617-624.
9. Barbosa-Cánovas, G.V., et al., *Food powders: physical properties, processing, and functionality*. Vol. 86. 2005: Springer.
10. Nampi, P.P., et al., *The effect of polyvinyl alcohol as a binder and stearic acid as an internal lubricant in the formation, and subsequent sintering of spray-dried alumina.* Ceramics International, 2011. **37**(8): p. 3445-3450.
11. Walton, D. and C. Mumford, *Spray dried products—characterization of particle morphology.* Chemical Engineering Research and Design, 1999. **77**(1): p. 21-38.
12. Crosby, E. and W. Marshall, *Effects of drying conditions on the properties of spray-dried particles.* Chemical Engineering Progress, 1958. **54**(7): p. 56-63.
13. Nandiyanto, A.B.D. and K. Okuyama, *Progress in developing spray-drying methods for the production of controlled morphology particles: From the nanometer to submicrometer size ranges.* Advanced powder technology, 2011. **22**(1): p. 1-19.
14. Santos, D., et al., *Spray drying: an overview*. Biomaterials-Physics and Chemistry-New Edition, 2018: p. 9-35.
15. Handscomb, C.S., M. Kraft, and A.E. Bayly, *A new model for the drying of droplets containing suspended solids.* Chemical Engineering Science, 2009. **64**(4): p. 628-637.
16. Jr Walker, W.J., J.S. Reed, and S.K. Verma, *Influence of slurry parameters on the characteristics of spray-dried granules.* Journal of the American Ceramic Society, 1999. **82**(7): p. 1711-1719.
17. Huang, L., K. Kumar, and A. Mujumdar, *Use of computational fluid dynamics to evaluate alternative spray dryer chamber configurations.* Drying Technology, 2003. **21**(3): p. 385-412.
18. Peighambardoust, S., A.G. Tafti, and J. Hesari, *Application of spray drying for preservation of lactic acid starter cultures: a review.* Trends in Food Science & Technology, 2011. **22**(5): p. 215-224.
19. *toppr answr*. 05.09.2022 17.12.2022]; Available from: https://www.toppr.com/ask/question/write-a-brief-account-of-electrostatic-precipitator-with-a-neat/.

20. Shabde, V., *Optimal design and control of a spray drying process that manufactures hollow micro-particles*. 2006, Texas Tech University.
21. Sarraf, H. and J. Havrda, *Rheological behavior of concentrated alumina suspension: Effect of electrosteric stabilization.* Ceramics Silikaty, 2007. **51**(3): p. 147.
22. Jr Walker, W.J., J.S. Reed, and S.K. Verma, *Influence of granule character on strength and Weibull modulus of sintered alumina.* Journal of the American Ceramic Society, 1999. **82**(1): p. 50-56.
23. Tsetsekou, A., et al., *Optimization of the rheological properties of alumina slurries for ceramic processing applications Part II: Spray-drying.* Journal of the European Ceramic Society, 2001. **21**(4): p. 493-506.
24. Zare, M.H., N. Hajilary, and M. Rezakazemi, *Microstructural modifications of polyethylene glycol powder binder in the processing of sintered alpha alumina under different conditions of preparation.* Materials Science for Energy Technologies, 2019. **2**(1): p. 89-95.
25. Anandharamakrishnan, C., *Handbook of drying for dairy products*. 2017: John Wiley & Sons.
26. Konsztowicz, K., et al., *ROLE OF SURFACE TENSION IN THE FORMATION OF DONUT-SHAPED GRANULES DURING SPRAY-DRYING.* Ceramic Transactions, 1991. **26**: p. 46-53.
27. Konsztowicz, K., et al., *EFFECT OF APPARENT SURFACE TENSION OF COLLOIDAL SUSPENSIONS ON THE SHAPE OF THE PRODUCTS OF SPRAY-DRYING.* Ceramic Transactions, 1991. **22**: p. 363-368.
28. Stunda-Zujeva, A., Z. Irbe, and L. Berzina-Cimdina, *Controlling the morphology of ceramic and composite powders obtained via spray drying–a review.* Ceramics International, 2017. **43**(15): p. 11543-11551.
29. Breinlinger, T., A. Hashibon, and T. Kraft, *Simulation of the influence of surface tension on granule morphology during spray drying using a simple capillary force model.* Powder Technology, 2015. **283**: p. 1-8.
30. Handscomb, C.S., *Simulating droplet drying and particle formation in spray towers*. 2009, University of Cambridge.
31. Ramavath, P., et al., *Effect of primary particle size on spray formation, morphology and internal structure of alumina granules and elucidation of flowability and compaction behaviour.* Processing and Application of Ceramics, 2014. **8**(2): p. 93-99.
32. Daraei, A., M. Nabipoor Hassankiadeh, and M. Golmohammadi, *Effect of Polyethylene Glycol (PEG) Powder on Compressibility and Microstructural Properties of Sintered α-Alumina.* Chemical Engineering Communications, 2016. **203**(1): p. 47-52.
33. Dhara, S. and P. Bhargava, *Influence of nature and amount of dispersant on rheology of aged aqueous alumina gelcasting slurries.* Journal of the American Ceramic Society, 2005. **88**(3): p. 547-552.
34. Jaafar, C., et al. *Effects of PVA-PEG binders system on microstructure and properties of sintered alumina*. in *Applied Mechanics and Materials*. 2014. Trans Tech Publ.
35. Davies, J. and J. Binner, *The role of ammonium polyacrylate in dispersing concentrated alumina suspensions.* Journal of the European Ceramic Society, 2000. **20**(10): p. 1539-1553.
36. Tsetsekou, A., C. Agrafiotis, and A. Milias, *Optimization of the rheological properties of alumina slurries for ceramic processing applications Part I: Slip-*

casting. Journal of the European Ceramic Society, 2001. **21**(3): p. 363-373.
37. Miller, J. *Measuring zeta potential - origin of zeta potential*. Mar 21, 2019; Available from: https://youtu.be/GjpSvKHMPB0.
38. CESARANO III, J. and I.A. Aksay, *Processing of highly concentrated aqueous α-alumina suspensions stabilized with polyelectrolytes.* Journal of the American Ceramic Society, 1988. **71**(12): p. 1062-1067.
39. Tjipangandjara, K.F., et al., *Correlation of alumina flocculation with adsorbed polyacrylic acid conformation.* Colloids and surfaces, 1990. **44**: p. 229-236.
40. Baklouti, S., et al., *The effect of binders on the strength and Young's modulus of dry pressed alumina.* Journal of the European Ceramic Society, 1998. **18**(4): p. 323-328.
41. Casson, N., *A flow equation for pigment-oil suspensions of the printing ink type.* Rheology of disperse systems, 1959.
42. Krieger, I.M. and T.J. Dougherty, *A mechanism for non-Newtonian flow in suspensions of rigid spheres.* Transactions of the Society of Rheology, 1959. **3**(1): p. 137-152.
43. Hotta, M., et al., *Powder layer manufacturing of alumina ceramics using water spray bonding.* Journal of the Ceramic Society of Japan, 2016. **124**(6): p. 750-752.
44. Taktak, R., S. Baklouti, and J. Bouaziz, *Effect of binders on microstructural and mechanical properties of sintered alumina.* Materials characterization, 2011. **62**(9): p. 912-916.
45. Sathish, S., et al., *Granulation of nano alumina powder for improved flowability by spray drying.* Transactions of the Indian Institute of Metals, 2012. **65**(5): p. 485-490.
46. Somton, K., et al., *The effect of granule morphology and composition on the compaction behavior and mechanical properties of 92% alumina spray dried granules.* Journal of Metals, Materials and Minerals, 2012. **22**(2).
47. Ghanizadeh, S., et al., *Spray freeze granulation of submicrometre alpha-alumina using ultrasonication.* 2016.
48. Baklouti, S., et al., *Young's modulus of dry-pressed ceramics: the effect of the binder.* Journal of the European Ceramic Society, 1999. **19**(8): p. 1569-1574.
49. Jr Walker, W.J., et al., *Adsorption behavior of poly (ethylene glycol) at the solid/liquid interface.* Journal of the American Ceramic Society, 1999. **82**(3): p. 585-590.
50. Naglieri, V., et al., *Optimized slurries for spray drying: Different approaches to obtain homogeneous and deformable alumina-zirconia granules.* Materials, 2013. **6**(11): p. 5382-5397.
51. Cottrino, S., et al., *Spray-drying of highly concentrated nano alumina dispersions.* Powder technology, 2013. **237**: p. 586-593.
52. Jafari, S.M., et al., *Nano spray drying of food ingredients; materials, processing and applications.* Trends in Food Science & Technology, 2021. **109**: p. 632-646.
53. Kang, S.-J.L., *Sintering: densification, grain growth and microstructure*. 2004: Elsevier.
54. Maury, M., et al., *Effects of process variables on the powder yield of spray-dried trehalose on a laboratory spray-dryer.* European Journal of Pharmaceutics and Biopharmaceutics, 2005. **59**(3): p. 565-573.